Title

Formulation and characterization of pressure-assisted microsyringe 3D-printed scaffolds for controlled intravaginal antibiotic release.

Authors

Kyser, Anthony

Mahmoud, Mohamed

Herold, Sydney

et al.

Publication Date

2023-06-25

DOI

10.1016/j.ijpharm.2023.123054

Peer reviewed

HHS Public Access

Author manuscript

Int J Pharm. Author manuscript; available in PMC 2024 June 25.

Published in final edited form as:

Int J Pharm. 2023 June 25; 641: 123054. doi:10.1016/j.ijpharm.2023.123054.

Formulation and Characterization of Pressure-Assisted Microsyringe 3D-Printed Scaffolds for Controlled Intravaginal Antibiotic Release

Anthony J. Kyser[a], **Mohamed Y. Mahmoud**[a,b], **Sydney E. Herold**[a], **Warren G. Lewis**[c,d], **Amanda L. Lewis**[c,d], **Jill M. Steinbach-Rankins**[a,e,f,g,†], **Hermann B. Frieboes**[a,e,f,h,†,*]

[a] - Department of Bioengineering, University of Louisville Speed School of Engineering, Louisville, KY 40202, USA

[b] - Department of Toxicology and Forensic Medicine, Faculty of Veterinary Medicine, Cairo University, Egypt

[c] - Department of Obstetrics, Gynecology and Reproductive Sciences, University of California San Diego, La Jolla, CA 92093, USA

[d] - Glycobiology Research and Training Center, University of California San Diego, La Jolla, CA 92093, USA

[e] - Department of Pharmacology and Toxicology, University of Louisville School of Medicine, Louisville, KY 40202, USA

[f] - Center for Predictive Medicine, University of Louisville, Louisville, KY 40202, USA

[g] - Department of Microbiology and Immunology, University of Louisville School of Medicine, Louisville, KY 40202, USA

[h] - UofL Health – Brown Cancer Center, University of Louisville, KY 40202, USA

Graphical Abstract

[*]Correspondence: Hermann B. Frieboes, Department of Bioengineering, Lutz Hall 419, University of Louisville, KY 40208, USA. Tel.: 502-852-3302; Fax: 502-852-6806; hbfrie01@louisville.edu.

[†] Joint senior authorship

CRediT STATEMENT

Anthony J. Kyser: Data curation; Formal analysis; Investigation; Validation; Visualization; Roles/Writing - original draft; Writing - review & editing

Mohamed Y. Mahmoud: Data curation; Formal analysis; Investigation; Visualization; Writing - review & editing

Sydney E. Herold: Data curation; Investigation

Warren G. Lewis: Formal analysis; Funding acquisition; Writing - review & editing

Amanda L. Lewis: Formal analysis; Funding acquisition; Writing - review & editing

Jill M. Steinbach-Rankins: Conceptualization; Formal analysis; Funding acquisition; Methodology; Project administration; Resources; Supervision; Writing - review & editing

Hermann B. Frieboes: Conceptualization; Formal analysis; Funding acquisition; Methodology; Project administration; Resources; Supervision; Writing - review & editing

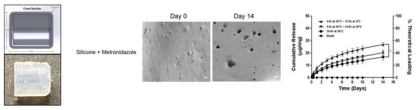

Abstract

Bacterial vaginosis (BV) is a highly recurrent vaginal condition linked with many health complications. Topical antibiotic treatments for BV are challenged with drug solubility in vaginal fluid, lack of convenience and user adherence to daily treatment protocols, among other factors. 3D-printed scaffolds can provide sustained antibiotic delivery to the female reproductive tract (FRT). Silicone vehicles have been shown to provide structural stability, flexibility, and biocompatibility, with favorable drug release kinetics. This study formulates and characterizes novel metronidazole-containing 3D-printed silicone scaffolds for eventual application to the FRT. Scaffolds were evaluated for degradation, swelling, compression, and metronidazole release in simulated vaginal fluid (SVF). Scaffolds retained high structural integrity and sustained release. Minimal mass loss (<6%) and swelling (<2%) were observed after 14 days in SVF, relative to initial post-cure measurements. Scaffolds cured for 24 hr (50°C) demonstrated elastic behavior under 20% compression and 4.0 N load. Scaffolds cured for 4 hr (50°C), followed by 72 hr (4°C), demonstrated the highest, sustained, metronidazole release (4.0 and 27.0 μg/mg) after 24 hr and 14 days, respectively. Based upon daily release profiles, it was observed that the 24 hr timepoint had the greatest metronidazole release of 4.08 μg/mg for scaffolds cured at 4 hr at 50°C followed by 72 hr at 4°C. For all curing conditions, release of metronidazole after 1 and 7 days showed >4.0-log reduction in *Gardnerella* concentration. Negligible cytotoxicity was observed in treated keratinocytes comparable to untreated cells, This study shows that pressure-assisted microsyringe 3D-printed silicone scaffolds may provide a versatile vehicle for sustained metronidazole delivery to the FRT.

Keywords

Gardnerella ; sustained release; metronidazole; 3D-printing; drug delivery; bacterial vaginosis; vaginal microbiome

1. Introduction

Bacterial vaginosis (BV) is prevalent in 23 to 29% of women of reproductive age, and studies have shown prevalence as high as 50% in high-risk populations[1–4]. The majority of women with BV are asymptomatic, yet they still have increased risks of sexually transmitted infections, cervical cancer, and pregnancy/fertility-related complications[5–13]. Furthermore, the current gold standard of treatment, in the form of antibiotics, can lead to a reduction in the number and species of beneficial bacteria in the vaginal microenvironment[14,15]. The elimination of beneficial as well as pathogenic bacteria has been associated with a higher likelihood of recurrent infections 6 or more months after treatment[16]. *Gardnerella vaginalis (Gardnerella)*, a predominant species seen in BV, has been shown to exist in multiple genomically distinct clades in patients[17,18]. These clades and activated DNA repair genes may pose challenges to antibiotic treatment and could lead to the proliferation of

antibiotic-resistant *Gardnerella*[19]. Moreover, the refractory nature of *Gardnerella* biofilms to treatment is likely to contribute to high rates of recurrence[20,21].

In addition to antibiotic-specific issues, distinct challenges are associated with oral and vaginal dosage forms used for administration. Oral antibiotics typically have lower absorption and lose potency through metabolism, while vaginally-applied topicals are challenged with drug solubility in vaginal fluid and lack of user adherence to frequent (often once-to-twice daily) treatment regimens[22–27]. Recommended antibiotics include metronidazole, tinidazole, and clindamycin[28], and depending on the drug type, oral regimens entail 0.1–2.0 grams/day for 2 to 7 days[26]. Two vaginal creams recommended by the Centers for Disease Control and Prevention (CDC) consist of either a 0.75% metronidazole or 2% clindamycin cream, administered for 5 or 7 days, respectively. Given the inherent challenges in antibiotic approaches, an alternative strategy is the oral or vaginal administration of beneficial bacteria, or probiotics, to help alleviate disturbances in vaginal health[29]. While probiotics alone have demonstrated some clinical success, a combination of probiotics as an adjunct therapy to antibiotic treatment has demonstrated a reduction in recurrent BV relative to antibioticonly treatment[30–35]. Yet, similar to antibiotic delivery, current probiotic dosage forms suffer from a lack of stability and challenges with user adherence to treatment regimens requiring frequent administrations[36,37].

In addition to sustaining or staging delivery, localized intravaginal delivery can help to bypass the gastrointestinal tract and hepatic first pass effect, increasing active agent concentration at the target site[38,39]. Localized sustained delivery increases bioavailability by ensuring a favorable drug presence can be absorbed throughout a prolonged period of time[39], which can help to mitigate issues inherent in achieving efficacy, including bioavailability and user adherence. For BV-specific applications, intravaginal administrations of metronidazole eliminated BV as effectively as orally-administered metronidazole, with less adverse effects[26]. In particular, single-dose applications of metronidazole vaginal vehicle gels (1.3%) have presented promising clinical outcomes while underscoring patient satisfaction due to the convenience of treatment administration[40]. Designed hydrogels composed of hyaluronic acid and metronidazole in the form of a film exhibited burst release of metronidazole with demonstrated film flexibility[41]. Similarly, metronidazole-containing chitosan hydrogels reduced the viability of *Trichomonas vaginalis* via extended release[42]. With hot melt extrusion (HME), poly(caprolactone) (PCL) matrices were developed with metronidazole and maleic acid in which the formulation demonstrated enhanced rapid dissolution profile while having improved sustained release for 7 days[43]. Diffusion mediated release of metronidazole from bigels enables their use as a potential delivery platform for antibiotic controlled delivery[44]. Polyvinylpyrrolidone vaginal nanofibers loaded with metronidazole exhibited rapid release of the majority of drug by 1 hr (hr)[45]. Innovation for localized delivery is evident; however, the superiority of 3D-printing for localized delivery of metronidazole is manifested by sustained and controlled release over a prolonged duration of time, mechanical strength, and versatility in design and drug concentrations.

While a variety of dosage forms have been developed to provide intravaginal delivery[38,46–48], few provide sustained release of small molecule drugs. Relative to existing

techniques, 3D-printing is a relatively new approach that has recently been applied to the design and development of intravaginal sustained release dosage forms. Recently, utilizing HME, polyurethane and clotrimazole were mixed and formed into a feed filament for fused deposition modeling (FDM) 3D-printing of intravaginal rings which demonstrated sustained release for 7 days[49]. Similarly, through the use of FDM 3D-printing, tunable controlled release of hydroxychloroquine, IgG, gp120 fragment, and coumarin 6 nanoparticles from polyurethane intravaginal rings was developed[50]. Additionally, HME followed by FDM 3D-printing of formulated filament containing progesterone, polyethylene glycol, polylactic acid, polycaprolactone, and tween has been formulated into various vaginal ring shapes for sustained release of progesterone[51]. Progesterone was also FDM 3D-printed with polyvinyl alcohol in the form of suppository molds[52]. In different forms, vaginal meshes were developed using FDM 3D-printing after HME of thermoplastic polyurethane and Levofloxacin for sustained antibiotic release after surgical implantation[53]. Very recently, the ratio of high and low molecular weight PCL was varied in 3D-printed vaginal discs by the method of semi-solid extrusion to evaluate the effect of polymer composition on sustained metronidazole release[54]. Using FDM printing, thermoplastic polyurethane filaments with metronidazole jellified with chitosan were developed into intravaginal rings that demonstrated reduction in concentration of *Escherichia coli*[55]. Selective laser sintering has also been utilized for its rapid drug release capabilities; with the 3D-pritning of metronidazole, it enabled the majority of metronidazole release under 4 hr[56]. With the versatility and variety of 3D-printing, oral and vaginal platforms loaded with metronidazole exhibit different release kinetics, underscoring the role and capabilities of 3D-printing to control drug release in addition to personalizing forms by altering the drug concentration.

3D-printing enables fine resolution and the design of architectures that exploit surface area to increase the ability of devices to sustain release[57]. Through customized dosing and formulations, 3D-printing can provide personalized treatment to a larger variety of populations[58]. Compared to molding techniques, pressure assisted microsyringe (PAM) 3D-printed constructs retain accurate shape fidelity, exhibit higher drug uniformity, and enable more accurate personalized dosing than molding[59]. Furthermore, molds demonstrate faster drug release compared to extruded prints[60], a disadvantage for sustained delivery applications. Additionally, PAM 3D-printing provides advantages over HME and FDM techniques when it comes to incorporating high drug concentrations, using a variety of materials, and maintaining drug stability via lower temperatures during fabrication[61,62].

Given these attributes, this study utilized PAM 3D-printing to fabricate silicone scaffolds that incorporate the antibiotic metronidazole. For other established sustained-release dosage forms, such as intravaginal rings, silicone has been used due to its favorable diffusivity and solubility coefficients for drug permeation[63]. Additionally, silicone has shown to be a biocompatible material based upon inflammation responses observed in in vivo studies[64]. The flexibility of silicone helps maintain specific constructs favorable for release and resist degradation/deformation via compression[65]. Through sustained delivery of metronidazole, these scaffolds are intended for pre-clinical evaluation via single-dose administration to the murine vaginal tract for 14 day use against vaginal microbiome-related infections, with the goal of future upscaling to human application. This study focuses on the characterization of PAM 3D-printed silicone integrated with metronidazole into the form of a shelled

cylindrical scaffold (diameter: 4 mm, length: 5 mm) with emphasis on material formulation, 3D-printing, curation relative to mechanical properties, and sustained release.

2. Materials and Methods

2.1. Materials

A mixture of vinyl terminated polydimethylsiloxane (70%) and vinyl, methyl modified silica (30%), and methylhydrosiloxane-dimethylsiloxane copolymer, trimethylsiloxane terminated was purchased from Allevi, Inc. (Philadelphia, PA). The drug, metronidazole, and dimethyl sulfoxide (DMSO) were obtained from Sigma Aldrich (St. Louis, MO). Acetic acid was obtained for incorporation for resolution refinements (Fisher, A38S-500). Simulated vaginal fluid (SVF) was prepared according to instruction from[66]. Phosphate buffer saline (PBS) composed of 137 mM NaCl (VWR, 0241-1kg), 2.7 mM KCl (Fisher, P217–500), 10 mM Na_2HPO_4 (Sigma, S9763-100G), and 1.8mM KH_2PO_4 (Sigma, P5655-100G) were purchased for use of washing scaffolds. Streptomycin-resistant clinical isolate of *Gardnerella* (strain JCP8151B, GenBank JX860320) was generously provided by Dr. Amanda Lewis (University of California San Diego, San Diego, CA). The CAD (computer-aided design) software SOLIDWORKS published by Dassault Systemes (Velizy-Villacoublay, France) was used to create scaffold design CAD parts that were converted to stereolithography (STL) files for 3D-printing.

2.2. Preparation of Ink

The Allevi 3 bioprinter (Allevi, Inc., PA) was used to print the prepared ink. The silicone was acquired from Allevi as two components with a 10:1 formulation ratio. The ratio consisted of a mixture of vinyl terminated polydimethylsiloxane (70%) and vinyl, methyl modified silica (30%) and methylhydrosiloxane-dimethylsiloxane copolymer, trimethylsiloxane terminated.

Due to the hydrophobic nature of metronidazole, DMSO was added to formulate a homogenous mixture with silicone for extrusion printing through the Allevi 3 bioprinter. The antibiotic, metronidazole, was ground, using a mortar and pestle, to a fine powder. Metronidazole (55 mg) was solubilized in 60 μL of DMSO and was subsequently added to the silicone ink. The ink was mixed in a 5 ml Eppendorf conical vial with a spatula until homogenous. With total volume of 1 ml, prepared ink was transferred into a syringe for 3D-printing. The ink was loaded with a metronidazole concentration of 50 μg/mg scaffold in order to obtain drug release previously shown to be effective[28,67]. The concentration was acquired by using the following equation (1) below:

$$Concentration = W_{Drug}/W_{Polymer} \quad (1)$$

Previous studies have shown that murine vaginal tracts measured at an average of 4 mm diameter and 5 mm depth[68], defining the dimensions for the scaffold. In contrast to ring form, a cylindrical form, similar to suppositories, was used to generate a greater surface area for release. Scaffold dimensions were 4 mm diameter, 5 mm height, and 0.5 mm shell thickness.

2.3. 3D-Printing Scaffold Structure

Printing parameters were optimized to produce the intended geometric design consistently. Due to thermosensitivity and shear thinning behavior of silicone, the temperature of the CORE head of the printer was adjusted to determine optimum temperature for favorable viscosity for extrusion[69]. Pressure was evaluated for consistent extrusion rate of ink. The thickness layer, extrusion rate, and infill distance were attuned to print the cylindrical scaffolds, sized for future pre-clinical murine application. An infill distance was utilized to print mechanically optimized cross-sectional slices of area per layer with intent of sustained release. The base polymer, a mixture of vinyl terminated polydimethylsiloxane (70%) and vinyl, methyl modified silica (30%), and curing agent, methylhydrosiloxane-dimethylsiloxane copolymer, trimethylsiloxane terminated, undergo a hydrosilylation reaction under high temperature exposure, a reaction commonly utilized with the fabrication of silicone elastomers for vaginal applications[70–73]. Metronidazole incorporation at concentrations of 10, 25, and 50 μg/mg scaffold were printed, and resolution of height and diameter were measured with calipers. With the addition of solvents, DMSO and acetic acid, scaffold resolution was measured at same concentrations.

Multiple post-print curing conditions were utilized to determine their potential effects on scaffold integrity. From preliminary mechanical characterization outcomes, three curing parameters were selected for further analysis. Scaffold curing of 4 hr at 50 °C was chosen to mitigate logarithmic reduction in viable counts of thermophilic species, in the case of incorporating biologics into the core of the scaffold[74,75]. Scaffold curing was followed by either 24 hr desiccation (20°C) or 72 hr refrigeration (4°C). Scaffold curing condition of 24 hr at 50°C was also utilized to strengthen mechanical integrity without necessarily incorporating biologics. Post-cure, the scaffolds were measured using a caliper to determine if the desired diameter (4 mm) and length (5 mm) were met accurately. Proper establishment was defined by fine resolution and the dimensions that matched the specified printing dimensions in the STL file.

2.4 Scaffold Physicochemical Characterization

Blank (without drug) and metronidazole (50μg/mg)-containing scaffolds cured under the different conditions underwent thermal analysis using thermogravimetric analysis (TGA) and differential scanning calorimetry (DSC) by utilizing SDT Q600 TA instrument (New Castle, DE) for simultaneous measurement of weight change and true differential heat flow. Scaffolds were cut into samples in range of ~15–20 mg and placed on ceramic cups. Samples were subsequently heated from 35 to 1000°C at a rate of 50°C/min., under flow of N_2 (100 mL/min). Data was extracted and analyzed using TA Universal Analysis software (New Castle, DE).

Fourier Transform Infrared Spectroscopy (FTIR) was used to identify the components of the formulated 3D-printed scaffolds. Blank and metronidazole-containing scaffolds cured under the different conditions were evaluated via FTIR. Infrared spectra were recorded on a JASCO FTIR spectrometer (Easton, MD), equipped with an attenuated total reflection (ATR) stage. Scans of spectra were collected in the range 400–4000 cm^{-1} at 4 cm^{-1} resolution.

2.5. Mass Swelling and Degradation

The initial mass was measured on a scientific scale with microgram sensitivity. Scaffolds were then placed in microcentrifuge tubes in 1 mL of SVF. Mass swelling was measured at following timepoints: 0, 4, 8, 24, 72, 120 hr, and 1,2,3, and 4 wk. Scaffolds were transferred into new 1 mL SVF following each timepoint. Before each measurement, excess solute was removed off surface of scaffolds and the scaffolds were weighed. The determination of mass swelling was dependent on the change in mass with respect to the initial mass and was calculated according to Eq.(1).

$$\text{Mass Swelling Percentage} = (W_s - W_i)/W_i \times 100 \quad (1)$$

Mass loss was calculated when replicates were initially weighed prior to immersion in SVF. At the specific timepoint of interest, scaffolds were removed from microcentrifuge tubes containing 1 ml SVF and dried at 50°C and were measured after 24 hr. Mass loss was determined by Eq.(2):

$$\text{Mass Loss Percentage} = (W_i - W_f)/W_i \times 100 \quad (2)$$

2.6. Compression Analysis

The vagina may be subjected to dynamic multiaxial loading, including continuing compression from the muscularis layer, vaginal wall stress and strain, vaginal wall prolapse as well as vaginal distension[76,77]. Scaffold mechanical integrity was evaluated using an Instron 5569 compression testing system. Extrapolation of load, strain, and stress was acquired using Instron Bluehill software (Norwood, MA). The load cell was 5kN and the force applied was set from 0.6 to 1.6 N. Displacement was set at 1 mm, or 20%, 25% compression load on axial and radially of scaffold, respectively, which was executed at compression rate of 1 mm/min.

2.7. Metronidazole Release

Loaded scaffolds containing 50 μg/mg of metronidazole were transferred into 1 mL conical vials containing SVF and placed in incubator at 37°C. The metronidazole release was evaluated at timepoints of 2, 4, 8 hr and 1, 2, 3, 4, 5, 6, 7, 8, 9, 10, and 14 days. The amount released per day was determined by reading absorbance of samples of supernatant (320 nm, Gen 5 app, BioTek Synergy H1 Microplate Reader). Metronidazole concentration was measured by ultraviolet–visible spectroscopy (UV–Vis) and determined by the validated calibration of $y = 0.0166x + 0.0301$, with $R^2 = 0.9953$. From acquiring the standard calibration curve, measuring the standard deviation of 5 blanks, and using limit of detection and limit of quantification equations[78], it was determined that the limits of detection and quantification were 3.00 μg/ml and 9.08 μg/ml, respectively. After each timepoint, excess SVF on the scaffold surface was carefully removed as supernatant and delicately dried, to ensure minimum drug loss prior to being placed into fresh 1 mL SVF.

2.8. Inhibition of *Gardnerella*

Gardnerella was cultured for 24 hr prior to inhibition studies in NYC III broth or agar media pre-equilibrated in an anaerobic chamber. Metronidazole release from 3D-printed scaffolds was evaluated to determine their potential to inhibit *Gardnerella* growth in the presence of VK2/E6E7 vaginal epithelial cells. Metronidazole-containing scaffolds cured 4 hr at 50°C followed by 24 hr desiccation (20°C) or 72 hr refrigeration (4°C), and scaffolds cured for 24 hr at 50°C were utilized. Supernatants from the scaffolds after 24 hr and 7 days in SVF were cultured with *Gardnerella* in NYC III.

Briefly, in a 48-well plate with each well containing confluent VK2/E6E7 cells and 250 μL of antibiotic-free cell media, 250 μL of each scaffold supernatant was added to each well in triplicates. The 48-well plate was then incubated in 5% CO2 at 37°C for 1 hr to give time for the supernatant to lower the media pH and thus provide protection for VK2 cells against *Gardnerella*. Afterward, 250 μL of free *Gardnerella* at 1×10^6 CFU/mL were added to each well and the 48-well plate was placed in anaerobic conditions at 37°C. After 24 hr incubation, each well was serially-diluted and 5 μL of each dilution was plated on corresponding MRS and NYC III agar plates incubated anaerobically at 37°C. After 48 hr incubation, colony forming units were counted for each dilution and the number of CFUs/mL was calculated. Controls as single experimental conditions included metronidazole alone (50 μg/ml) in culture with *Gardnerella*, and free *Gardnerella* at 1×10^6 CFU/mL with supernatants from blank scaffolds (containing no bacteria). Viability was determined as the log-decrease relative to the free *Gardnerella* CFU count for that sample group, at each corresponding time point.

2.9. SEM Imaging

The morphology of the blank and metronidazole-containing scaffolds was characterized using scanning electron microscopy (SEM). Samples of scaffold cross-sections and surfaces were placed on carbon tape, sputter-coated with a layer of palladium/gold alloy (8.5 nm) and imaged using Apreo C LoVac Field Emission SEM (Thermo Scientific, Waltham, MA). Porosity was compared in scaffolds that were immersed in timepoints at 0 and 14 days in SVF. Image J (NHI LOCI, University of Wisconsin) was utilized to evaluate scaffold area and porosity size.

2.10. VK2/E6E7 Viability

An MTT (3-(4,5-dimethylthiazol-2-yl)-2,5-diphenyl-2H-tetrazolium bromide) assay was used to determine the preliminary *in vitro* safety of DMSO and cured silicone, blank and metronidazole-containing scaffolds, in a VK2/E6E7 cell line. Cells were plated at a density of 300,000/well in a 12-well plate and incubated for 24 hr at 37°C. Media only (untreated cells) and 10% DMSO were used as viable and non-viable cell controls. After 24 and 72 hr incubation, 100 μL of MTT labeling reagent was added to each well and incubated at 37°C for 4 hr, followed by addition of 100 μL of lysis buffer containing 10% sodium dodecyl sulfate and 0.01 M hydrochloric acid. After 16 hr incubation, the absorbance was read at 570 nm (SYNERGY Microplate Reader, Biotek Instruments Inc) and normalized to cell-only absorbance to attain the relative percent of cell viability. For comparison, 10% DMSO was used as positive control, and VK2 cells only were used as negative control. In addition to the

formulated scaffolds, silicone with only DMSO and a blank scaffold were evaluated as well as metronidazole alone.

2.11. Lactic Dehydrogenase (LDH) Release Assay

Release of cytosolic enzyme LDH was measured using CytoTox96® non-radioactive cytotoxicity assay (Promega, Madison WI) to estimate loss of membrane integrity and resulting leakage of cellular contents. VK2/E6E7 cells were plated (300,000 cells in 1 mL media per well in 12-well flat bottom plate) and incubated for 24 hr at 37 °C, 5% CO2. Blank and metronidazole-containing scaffolds were added to cells in triplicate at 37 °C in 5% CO2 for 24 h and 72 hr. Supernatant (50 μl) from treated cells was added to LDH substrate and incubated at RT for 30 min. Reactions were terminated by adding 50 μL of stop solution. LDH activity was determined by measuring solution optical density at 490 nm. As controls, cells were treated with 1 ng of staurosporine (positive) or with medium only (negative). LDH release was calculated as percentage absorbance of each sample relative to negative controls.

2.12. Statistical Analysis

GraphPad (GraphPad Software, La Jolla, CA) was used for statistical analysis. All statistical analyses in GraphPad Prism (version 9.3.1) were performed using one-way ANOVA with Tukey HSD post-hoc comparisons ($p \leq 0.05$).

3. Results

3.1. Optimized formulation

The 10:1 w/w silicone:curing agent ink, containing 5% DMSO, was loaded with metronidazole concentration of 50 μg/mg scaffold. Resulting ink was 3D-printed into the cylindrical scaffold design for metronidazole release. The cylindrical geometric CAD design was developed using SOLIDWORKS and converted into a STL file for 3D-printing. Reproducibility of scaffold dimensions in 3D-printed scaffold are shown in Figure 1.

3.2. 3D-Printing Optimization and Resolution

Printing parameters were determined by evaluating printing resolution of metronidazole-containing scaffolds. Blank 10:1 scaffolds were 3D-printed with adjusted printing parameters, and the resulting scaffold dimensions were measured. First, the effect of adjusting pressure on extrusion for 3D-printing was evaluated (Figure 2A). Printing a height of 5 mm, 100 psi produced an accurate height of 5.05±0.04 mm whereas 80 psi produced a statistically significant ($p \leq 0.0001$) scaffold height of 2.59±0.40 mm. There was not a statistically significant difference in diameter sizes from the control, which had the desired CAD dimensions. Next, the effect of adjusting the CORE head temperature on 3D-printing scaffolds was evaluated (Figure 2B) where 30°C enabled the silicone ink to 3D-print scaffold height and diameter of 5.04±0.06 and 4.03±0.01 mm, respectively. Additionally, it was found that the 23G needle provided the best resolution for the silicone material with an optimized temperature and pressure of 30 °C and 100 psi.

A PAM 3D-printer provides constant extrusion, in contrast to single droplets, and a range of usable materials due to viscosity tolerance[79]. Extrusion rates were evaluated to determine a rate that provided the optimum resolution of each printing slice contingent on the ink viscosity. An extrusion rate of 5 mm/sec was observed to produce the most desirable dimensions of 5.02±0.06 and 4.09±0.07mm for height and diameter, respectively (Figure 2C). Improper slice printing due to the other extrusion rates, 2.5 and 7.5 mm/sec, resulted in statistically significant differences in scaffold height. Lastly, it was determined that a thickness layer of 0.2 mm provided the best scaffold resolution (Figure 2D). Thickness layer altered support of the structure as well as flexibility, as a smaller layer size increased the flexibility of the scaffold[80]. As thickness layer increased, both scaffold height and diameter resulted in statistically significant changes from the desired height and diameter. The zig-zag grid template produced the most desirable scaffold for the design of the scaffold and an infill distance of 0.35 mm removed ink overlap for each layer.

3.3 Metronidazole Incorporation and Resolution

To incorporate metronidazole and enable 3D-print through extrusion, a well-mixed ink was attained by partial dissolution of metronidazole. The solvents dimethyl sulfoxide (DMSO) and acetic acid were chosen as candidates for improving consistent ink extrusion. The resolution of prints created from silicone ink, silicone and 5% DMSO, and silicone and 5% acetic acid were evaluated at different metronidazole concentrations of 10, 25, and 50 μg/mg scaffold (Figure 3). The formulation of silicone with DMSO provided consistent print heights of 4.98±0.02, 4.96±0.04, and 5.04±0.04 mm corresponding with the metronidazole concentrations of 10, 25, and 50 μg/mg, respectively. Additionally, as the metronidazole concentration increased, the deviation in diameter increased for silicone and silicone and 5% acetic acid formulations, signifying less accuracy in diametric resolution. In contrast to these formulations, silicone ink containing 5% DMSO showed no deviation or statistical significance through all of the different loadings of metronidazole. Silicone ink containing 5% DMSO produced scaffolds with the optimum resolution.

3.4 Scaffold Physicochemical Characterization

Thermal analysis, scaffold phase changes, and weight loss were evaluated via TGA and DSC. All blank and metronidazole-containing scaffolds exhibited <5% weight loss below 250°C (Figure 4A). Weight loss behavior between blank and metronidazole-containing scaffolds began to deviate, and metronidazole-containing scaffolds began to have more prominent weight loss compared to blanks, when temperature reached ~550°C. Metronidazole-containing scaffolds lost 50% of their weight at ~750°C. In contrast to metronidazole-containing scaffolds, blank scaffolds did not exhibit a pronounced decrease in weight loss. By 800°C, these scaffolds had stabilized at 20% weight loss, further suggesting that incorporation of metronidazole and DMSO and their subsequent chemical interactions with the silicone base polymer and crosslinking agent influence the temperature stability of the scaffolds at higher temperatures. Minimal differences were observed between scaffold curing conditions.

Heat flow through the scaffolds measured via DSC exhibited endothermic behavior that corresponded to the weight loss (Figure 4B), with similar trends between blank and drug-

loaded scaffolds. Upon closer analysis of the first derivative of the heat flow (Figure 4C and D), both blank and metronidazole-containing scaffolds showed an endothermic peak at ~75°C. Metronidazole-containing scaffolds with cures 4 hr at 50°C followed by 72 hr at 4°C or 4 hr at 50°C followed by 24 hr in desiccation at 20°C had corresponding endothermic peaks to the pure metronidazole at ~161°C, albeit with melting point depression presence. However, given the lesser concentration of metronidazole (<5%,) relative to the whole formulation, the peaks were less prominent in comparison to pure metronidazole. Interestingly, a shift in endothermic peak for the scaffolds cured for 24 hr at 50°C at ~164°C may indicate that a higher degree of crosslinking alters the loaded metronidazole physicochemical properties, as also observed with their reduced metronidazole release in comparison to the other curing conditions. Past 700°C, broad endothermic peaks (Figure 4D) correspond to the sharp decreases of crosslinked polymeric decomposition observed in the TGA.

Scaffolds underwent FTIR analysis to confirm their identity. The absorbance peaks were very similar between blank and metronidazole-containing scaffolds (Supplementary Figure 1), indicating that the low overall metronidazole (<5% of bioink mass) amount did not noticeably affect the overall absorbance. In light of this, the curing conditions for blank and metronidazole-containing scaffolds exhibited similar polysiloxane bands for identifying the base polymer, a mixture of vinyl terminated polydimethylsiloxane (70%) and vinyl, methyl modified silica (30%), and crosslinking agent, methylhydrosiloxane-dimethylsiloxane copolymer, trimethylsiloxane terminated. FTIR spectra showed a sharp band at ~1260 cm^{-1} denoting the presence of functional group $Si\text{-}CH_3$ and accompanied by a strong band at ~785 cm^{-1}, both found in polysiloxanes. A sharp band at ~1010 cm^{-1} indicated presence of $Si\text{-}CH{=}CH_2$, another functional group present in the base polymer. Lower peaks such as the weak band at ~860 cm^{-1} are found in dimethylsiloxane copolymers such as the crosslinking agent used here. These bands were similarly detected and observed in previous compilation studies of organosilicon compounds[81].

3.5. Scaffold Swelling and Degradation as a Function of Curing

Mass swelling and degradation were evaluated to determine which curing condition would result in the least amount of absorbance of mass loss. Through 14 days, blank and metronidazole-containing scaffolds were immersed in SVF and shown to retain structure and remain intact (Figure 5A). Blank and metronidazole-containing scaffolds showed minimal swelling (<2%) for all curing conditions. Likewise, there was minimal degradation of the scaffolds (<6%) for all the curing conditions. There was not a significant difference between the blank and metronidazole-containing scaffolds for both swelling and degradation measurements (Figure 5B and C).

3.6. Compression Testing

Mechanical testing was performed on scaffolds at different cures to determine strength during administration and its residence in the vaginal canal. Compression testing was performed axially to simulate one-time, self-insertion of scaffold and radially to simulate physiological vaginal compression on scaffolds. None of the scaffolds reached yield strength nor fracture in stress/strain. After the 3D-printed scaffolds post-cure, scaffolds cured for 24

hr at 50°C demonstrated superior mechanical strengths compared to other curing conditions in the axial compressions for the blank and metronidazole-containing scaffolds (Figure 6A–B). It was observed that after these scaffolds had been immersed in SVF for 14 days, there was an increase in mechanical strength when cured for 4 hr at 50°C (Figure 6C–D).

3.7. Metronidazole Cumulative Release

Scaffolds cured for 4 hr at 50°C followed by 72 hr at 4°C showed the greatest cumulative release 27.0 μg/mg (54.1% theoretical loading) for the 14 day span (Figure 7). Based upon daily release profiles, it was observed that the 24 hr timepoint had the greatest metronidazole release of 4.08 μg/mg for scaffolds cured at 4 hr at 50°C followed by 72 hr at 4°C. All parameters displayed similar behavior of drug release, both cumulatively and daily. There were minimal changes in amount of drug release after Day 5 for all parameters.

3.8. Inhibition of *Gardnerella*

To evaluate the ability of the 3D-printed scaffolds to inhibit *Gardnerella*, supernatant from scaffolds 50μg/mg concentration of metronidazole was added to culture with *Gardnerella*. Supernatants were cultured with *Gardnerella* at concentrations (10^6 CFU/mL) for 24 hr under anaerobic conditions at 37°C. Figure 8 shows that *Gardnerella* viability was significantly ($p \leq 0.0001$) reduced by 4.18-, 4.51-and 4.62-log in the presence of 24 hr release supernatants from metronidazole-containing scaffolds cured for 24 hr at 50°C, cured 4 hr at 50°C followed by 24 hr desiccation (20 °C), or cured at 4 hr at 50 °C followed by 72 hr refrigeration (4°C), respectively. Similarly, *Gardnerella* viability was significantly ($p \leq 0.0001$) decreased in the presence of 7 day release supernatants from metronidazole-containing scaffolds cured for 24 hr at 50°C, cured 4 hr at 50°C followed by 24 hr desiccation (20 °C), or cured at 4 hr at 50 °C followed by 72 hr refrigeration (4°C) by 4.08-, 4.24-and 4.35-log, respectively.

3.9. SEM Imaging

Cross sections of blank and metronidazole containing scaffolds were imaged with SEM (Supplementary Figure 2). Through the software, ImageJ, scaffolds demonstrated an increase in porosity corresponding to the drug release. An increased porosity demonstrates the potential for biologic incorporation into core with subsequent release through the pores. Metronidazole-containing scaffolds demonstrated 0.73±0.08 % area of pores immediately after printing and 5.12±0.12 % area of pores after 14 days. Metronidazole-containing scaffolds with DMSO showed significantly ($p \leq 0.05$) lower % area of pores with 0.57±0.05 immediately after printing and 4.62 ± 0.18 after 14 days compared to scaffolds without DMSO.

3.10. Cell Viability and LDH Release

Since DMSO was used as the dissolution solvent for metronidazole, this study tested for cytotoxicity because of DMSO's potential to cause adverse reactions in cells[82]. Viability of vaginal keratinocytes (VK2/E6E7) was evaluated after treatment with blank and metronidazole-containing scaffolds (Figure 9A). Vaginal keratinocyte viability was maintained after 24 and 72 hr treatment with all ink formulation additions to the scaffold,

relative to untreated VK/E6E7 cells. The final formulated metronidazole-containing scaffolds maintained greater than 98.5% cell viability over 24 and 72 hr treatment conditions. In contrast, cell viability for negative control group, 10% DMSO, had viability of less than 35% and 28 of that observed with untreated cells over 24 and 72 hr. LDH release was measured as a marker for cell membrane integrity after treatment with blank and metronidazole-containing scaffolds (Figure 9B). LDH released from cells treated with all scaffolds was negligible relative to control untreated cells. However, LDH released from cells treated with staurosporine was significantly ($p \leq 0.0001$) higher than control or treated cells, indicating that scaffolds did not compromise cell membrane integrity.

4. Discussion

Antibiotics, such as metronidazole, clindamycin, and tinidazole, are recommended as the primary treatment for BV[28]. However, recurrence and antibiotic resistance may result from failure to achieve inhibitory concentrations, partially due to lack of user adherence because of frequent and inconvenient administration[18]. In this study, sustained metronidazole release from pressure-assisted microsyringe 3D-printed silicone scaffolds was evaluated with the goal to address these issues via local, sustained delivery of drug while retaining delivery vehicle biocompatibility. The burden of recurrent BV hinders personalized patient care and impacts underserved populations[3,4,83,84]. The emergence of 3D-printing provides an alternative to meet the growing demands of healthcare systems through tailored, individualized treatments[85–87]. Through 3D-printing, inks loaded with different drug concentrations offer the potential to meet patient health needs and achieve necessary inhibitory concentration to eliminate BV. Additive manufacturing provides for customized architectures to fine tune drug release[58,88–90]. Different geometrics offer mechanical strength and controlled drug delivery, to locally target BV. Formulating an ink is a multifaceted task involving consideration of resident biomaterial, active pharmaceutical ingredient (API) loading, and feasibility of manufacturing. The superiority of 3D-printing to develop a localized intravaginal delivery platform is further underscored by these manufacturing needs. In this study, PAM 3D-printing was considered was best suited to meet these criteria and provided a means to construct customized scaffolds to enhance and fine tune metronidazole release for female reproductive tract applications. Silicone has demonstrated biocompatibility in numerous applications. For vaginal applications, studies have shown multiple silicone-based drug delivery systems applied in the vaginal canal[91–95]. Favorable diffusion of drug from silicone has been shown to provide effective release kinetics[96–102].

The scaffold design in this study corresponds with murine vaginal tracts measured in previous studies[68]. As challenges arise from initial burst or sub-optimal release, the geometric design of a chamfered cylindrical scaffold was utilized to enhance and fine tune sustained release[57,94,103,104]. Through the use of 3D-printing, the specified CAD design was translated into silicone scaffolds with and without metronidazole, with reproducible dimensions (Figure 1). A shell interior with a wall thickness of 0.5 mm was created with the aim of incorporating future biologics into the core of the scaffold. To attain these reproducible dimensions for favorable release profiles, printing processing parameters of the used extrusion printer were evaluated for their impact on the height and diameter of the

printed cylindrical scaffolds. Layer thickness, temperature, and extrusion rate in conjunction with pressure have shown to impact drug delivery performance and physicochemical properties in 3D-printing[105]. Proper extrusion, using a 23 needle G, produced scaffold geometrics with least deviation from the control of height and diameter (5 and 4 mm) at 100 psi (Figure 2). When needle gauge size increases (decrease in diameter), as with extrusion rate, shear stress on the ink increases[106]. Adjusting the temperature of the CORE head changes the volume of bioink extruded for a given extrusion rate due to non-Newtonian shear thinning behavior of silicone and its changes in viscosity[69,107]. Changes in temperature of ink during extrusion were also assessed. Changes in viscosity as a result of different temperature produced statistically significant differences in height and diameter for temperatures, 15 and 45°C, indicating 30°C to obtain well-defined scaffolds. Additionally, drug dissolution and release have shown to be altered by extrusion rate and layer thickness that the subject is printed at[88]. It was observed that an extrusion rate of 5 mm/sec and a thickness of 0.2 mm provided the optimum scaffold construct. As thickness layer increased, it was observed that there was statistically significant increase in diameter, suggesting that the 3D-printed scaffold could not support resolution of a well-defined construct past 0.2 mm. A comparable work utilizing pressure assisted microsyringe 3D-printing to develop a shell construct for oral applications previously indicated how extrusion printing parameters have dire implications on release modulation[108]. In contrast with different types of 3D-printing, PAM relies on these particular printing parameters to fabricate well-defined architectures. Resolution of the prints is crucial for the intended release profile[88].

Once optimum printing parameters were determined, different formulations were utilized to evaluate resolution at different metronidazole concentrations of 10, 25, and 50 μg/mg scaffold. Lack of homogeneity in ink resulted in less defined scaffold production evident in Figure 3. Along with solely silicone ink, silicone inks with the addition of DMSO and acetic acid were evaluated. As higher metronidazole concentrations were loaded, both the silicone ink independent of the added solvent and silicone with 5% w/w of acetic acid resulted in statistically significant changes from the blank scaffold measurements at 50 μg/mg, indicating that these inks would hinder reproducible dimensions. Without the addition of polar solvents, the silicone ink showed a drop in resolution in height and diameter. The ink containing 5% w/w DMSO showed effective reproducible resolution capabilities, demonstrating its homogeneity through various drug concentrations.

3D-printed scaffolds underwent weight loss analysis by TGA as well as thermal analysis by DSC to confirm melting point of the incorporated drug metronidazole and crystallization of the scaffold material. It is evident that incorporation of metronidazole and DMSO alters the stability of the 3D-printed scaffolds at higher temperatures (>550°C) (Figure 4A). In the case of fabricating these scaffolds through a heated printing head at 30°C, scaffold stability remained intact as weight loss (>5%) is not evident until >250°C. Corresponding to TGA, heat flow from DSC for metronidazole-containing scaffolds exhibited endothermic peaks with a melting point depression of metronidazole, which has been observed in similar metronidazole-containing intravaginal devices[43] (Figure 4C). This shift potentially induces a point defect in crystallinity that may reduce intermolecular strength, also observed with the weight loss at higher temperature. Additionally, broad endothermic peaks past 700°C correspond to the sharp decline in weight loss observed in TGA (Figure 4D). Spectra

collected from FTIR sampling confirm identities of the base polymer and crosslinking agent for the hydrosilylation reaction (Supplementary Figure 1). Stretching of functional groups present in metronidazole had very weak intensity due to the low concentration of drug in the scaffolds.

Once the effective formulation was attained, blank and metronidazole-containing 3D-printed scaffolds underwent swelling and degradation evaluations. Swelling of material can alter the drug release kinetics, resulting in an initial burst instead of sustained release and also alter the mechanical integrity[109–111]. Degradation of the well-defined geometric architecture would also affect the release profile due to change of surface area. In this study, it was visually evident that both blank and scaffolds loaded with metronidazole concentration of 50 μg/mg had no traces of compromised architecture (Figure 5A). Measurements indicated minimal swelling (<2%) and degradation (<6%) across all curing conditions evaluated in blank and metronidazole-containing scaffolds indicating negligible effect on release efficacy (Figure 5B and C). These results demonstrate the ability of silicone to withstand physicochemical interactions with SVF that could be detrimental to their application. Furthermore, API incorporation into silicone has been demonstrated to be an effective platform for drug delivery for applications to the female reproductive tract.[63]

The scaffold would be subjected to compression when inserted in the vagina and would be further subjected to compression intra-vaginally from vaginal fluid, vaginal walls, and muscularis layer[53,76,112,113]. Scaffolds were mechanically tested post-cure and after 14 day in SVF to simulate initial insertion and residual duration, respectively (Figure 6). In comparison to the post-cure mechanical strengths, the 24 hr at 50°C cure demonstrated superiority over the other cures with regards to resistance to compression. In contrast, scaffolds cured for 4 hr at 50°C showed greater resistance to compression compared to 24 hr at 50°C cure when immersed in SVF, suggesting that scaffolds cured for lesser time would strengthen from vaginal fluid presence. Yet, these scaffolds had minimal swelling and degradation indicating SVF absorption was not occurring, consistent with previous observations[114].

The scaffolds were evaluated for cumulative release of metronidazole in SVF for 14 days. Scaffolds cured for 4 hr at 50°C followed by 72 hr at 4°C, had the greatest cumulative release (27.0 μg/mg) (Figure 7A). Independent of curing condition, the scaffolds released at minimum ~1 μg/mg per day over 7 days (Figure 7B), demonstrating the ability for sustained release. The degree of crosslinking polymers as well as curation period has been shown to impact drug release kinetics and mechanical strength[115–120]. Recently, we evaluated the drug release kinetics of 3D-printed scaffolds with these curing conditions, finding that the Higuchi, Korsmeyer-Peppas, and Peppas-Sahlin models adequately (all $R2$ ≥0.99) described the release, implying similarity to release from insoluble or polymeric matrices[114]. In this study, the metronidazole-containing scaffold cured at 4 hr at 50C followed by 72 hr at 4°C showed a statistically significant increase in cumulative release compared to the scaffolds cured for 24 hr at 50 °C, as well as statistically significant increase in resistance to compression after being immersed in SVF for 14 days, indicating this scaffold cure having the most advantageous sustained release and mechanical strength for 14 days *in vitro*. Regarding poor retention time of drugs in the vaginal mucosa, repeated

administration of a therapeutically retained concentration as well as mucoadhesive gels have been alternative solutions[121,122] . Mucoadhesive materials provide greater surface contact at the localized mucosal site for an increased drug flux at the absorbing tissue[123]. However, lack of user adherence due to inconvenient administration along with a transient effect may enhance the risk of antibiotic-resistant pathogenic growth. Sustained release through 3D-printing via a one-time insertion provides a solution to poor drug retention without potentially compromising user adherence. Additionally, the dimensions of the scaffolds, and their ability to withstand compression while retaining shape, offers the opportunity for prolonged vaginal retention, which will be evaluated in upcoming *in vivo* studies.

Supernatants from scaffolds cured at the various conditions were utilized in a prevention assay in the presence of VK2/E6E7 vaginal epithelial cells with *Gardnerella*. The release of metronidazole after 1 and 7 days showed greater than 4.0-log reduction in *Gardnerella* concentration ($P \leq 0.0001$) for all three scaffold cures (Figure 8). Metronidazole release for all scaffold cures was greater than 225 and 85 μg/ml for 1 and 7 days, respectively. Although the drug release did not reach equilibrium, the results indicate that the sustained release would logarithmically reduce colonies of *Gardnerella*[28]. Of note, the one-time administration dosage is designed for 14 day delivery of metronidazole.

Cross sections of scaffolds were imaged under SEM to determine the porosity after immersion in SVF. The presence of porosity was shown distributed throughout the scaffold area (Supplementary Figure 2). Pore sizes were observed to have a range of 5–20 μm suggesting the formulation could enable future proliferation of biologics from the core. Specifically, the pore size range would provide the ability for lactobacilli species to proliferate outward[124]. Similar findings of increased porosity within a 3D-printed polymeric construct after exposure to SVF for 14 days indicated the suitable use of silicone for sustained release of hydrophobic drugs[51]. Interestingly, the increase in porosity did not weaken the scaffold constructs; in fact, the mechanical strength increased during radial compression after 14 days in SVF compared to the initial strength observed in previous work[114]. This phenomenon is hypothesized to occur due to the increased surface area exposure to SVF, which may result in molecular interaction between uncrosslinked molecules. Lastly, the scaffolds were administered for 24 and 72 hr to vaginal keratinocytes (VK2/E6E7) to determine cell viability. Negligible cytotoxicity was observed in treated keratinocytes compared to untreated cells, indicating preliminary safety of the formulated scaffolds for intravaginal application (Figure 9). Minimal cytotoxicity and LDH release, in addition to the scaffold efficacy against *Gardnerella*, indicates that the presence of 5% w/w DMSO in the formulated ink did not impact cell viability.

The delivery platform evaluated in this study has the potential to be scaled up for human use. Metronidazole has been previously shown to eliminate *Gardnerella* without reducing commensal populations such as *L. crispatus* at a concentration of 50 μg/mg, by comparison of their MIC (μg/ml) values against metronidazole[28]. In light of this knowledge and the potential to incorporate biologics in the 3D-printed scaffolds[125] for a future dual antibiotic-probiotic delivery system, the ink formulation was composed of a metronidazole concentration of 50 μg/mg, and the architecture was shelled for potential inclusion of the biologics. The silicone and curing agent, a mixture of vinyl terminated polydimethylsiloxane

(70%) and vinyl, methyl modified silica (30%) and methylhydrosiloxane-dimethylsiloxane copolymer, trimethylsiloxane terminated, was mixed with 5% DMSO w/w to enable consistent extrusion with metronidazole. Future work will entail evaluating the stability and shelf-life of the scaffold, as well as the pharmacological efficacy and sustained retention *in vivo*.

Conclusions

This study demonstrates the potential of PAM 3D-printing as a versatile additive manufacturing process for creating metronidazole-containing silicone scaffolds that offer controlled and sustained metronidazole release, shown to logarithmically reduce the concentration of pathogenic colonies of *Gardnerella*. Scaffolds had minute changes during degradation and swelling as well as mechanical resistance to simulated self-insertion and circumferential forces present in the vaginal canal. Preliminary safety studies showed that vaginal cell viability was maintained, and images of porosity established the potential use of incorporating biologics into the core of the scaffolds for subsequent release after antibiotic release. The single-dose application scaffold could provide a convenient alternative for localized active agent delivery for 14 day sustained treatment, at which time the spent scaffold would be removed and, if needed, replaced with another unit. Altogether, this work is envisioned to contribute and facilitate a streamlined approach to develop extrusion-based 3D-printed constructs for localized and sustained intravaginal delivery of active agents to treat disturbances in vaginal health.

Supplementary Material

Refer to Web version on PubMed Central for supplementary material.

ACKNOWLEDGEMENTS

Authors gratefully acknowledge Dr. Noppadon Sathitsuksanoh for generously allowing use of the FTIR, and the Conn Center for Renewable Energy Research for the resources to perform thermal analysis of the 3D-printed samples.

This work was partially supported by National Institutes of Health / National Institute of Allergy and Infectious Diseases grant R01AI168475 (H. Frieboes / A. Lewis).

Abbreviations:

API	Active pharmaceutical ingredient
ATR	Attenuated total reflection
BV	Bacterial vaginosis
CAD	Computer-aided design
CDC	Centers for Disease Control and Prevention
DMSO	Dimethyl sulfoxide
DNA	Deoxyribonucleic acid

DSC	Differential scanning calorimetry
FDM	Fused deposition modeling
FTIR	Fourier transform infrared spectroscopy
HME	Hot melt extrusion
LDH	Lactic dehydrogenase
MIC	Minimum inhibitory concentration
MTT	3 -(4,5-dimethylthiazol-2-yl)-2,5-diphenyl-2H-tetrazolium bromide
PAM	Pressure assisted microsyringe
PBS	Phosphate-buffered saline
PCL	Ppoly(caprolactone)
SEM	Scanning electron microscopy
SVF	Simulated vaginal fluid
TGA	Thermogravimetric analysis
UV-Vis	Ultraviolet–visible spectroscopy

References

1. Workowski KA & Bolan GA Sexually transmitted diseases treatment guidelines, 2015. MMWR Recomm Rep 64, 1–137 (2015).
2. Peebles K, Velloza J, Balkus JE, McClelland RS & Barnabas RV High Global Burden and Costs of Bacterial Vaginosis: A Systematic Review and Meta-Analysis. Sex Transm Dis 46, 304–311, doi:10.1097/olq.0000000000000972 (2019). [PubMed: 30624309]
3. Kenyon C, Colebunders R & Crucitti T The global epidemiology of bacterial vaginosis: a systematic review. Am J Obstet Gynecol 209, 505–523, doi:10.1016/j.ajog.2013.05.006 (2013). [PubMed: 23659989]
4. Bautista CT et al. Bacterial vaginosis: a synthesis of the literature on etiology, prevalence, risk factors, and relationship with chlamydia and gonorrhea infections. Mil Med Res 3, 4, doi:10.1186/s40779-016-0074-5 (2016). [PubMed: 26877884]
5. Koumans EH et al. The prevalence of bacterial vaginosis in the United States, 2001–2004; associations with symptoms, sexual behaviors, and reproductive health. Sex Transm Dis 34, 864–869, doi:10.1097/OLQ.0b013e318074e565 (2007). [PubMed: 17621244]
6. Brotman RM et al. Bacterial vaginosis assessed by gram stain and diminished colonization resistance to incident gonococcal, chlamydial, and trichomonal genital infection. The Journal of infectious diseases 202, 1907–1915, doi:10.1086/657320 (2010). [PubMed: 21067371]
7. Wiesenfeld HC, Hillier SL, Krohn MA, Landers DV & Sweet RL Bacterial vaginosis is a strong predictor of Neisseria gonorrhoeae and Chlamydia trachomatis infection. Clin Infect Dis 36, 663–668 (2003). [PubMed: 12594649]
8. Leitich H & Kiss H Asymptomatic bacterial vaginosis and intermediate flora as risk factors for adverse pregnancy outcome. Best Pract Res Clin Obstet Gynaecol 21, 375–390, doi:10.1016/j.bpobgyn.2006.12.005 (2007). [PubMed: 17241817]

9. DiGiulio DB et al. Prevalence and diversity of microbes in the amniotic fluid, the fetal inflammatory response, and pregnancy outcome in women with preterm pre-labor rupture of membranes. Am J Reprod Immunol 64, 38–57, doi:10.1111/j.1600-0897.2010.00830.x (2010). [PubMed: 20331587]
10. Svare JA, Schmidt H, Hansen BB & Lose G Bacterial vaginosis in a cohort of Danish pregnant women: prevalence and relationship with preterm delivery, low birthweight and perinatal infections. BJOG 113, 1419–1425, doi:BJO1087 [pii]10.1111/j.1471-0528.2006.01087.x (2006). [PubMed: 17010117]
11. Kovachev SM Cervical cancer and vaginal microbiota changes. Archives of Microbiology 202, 323–327, doi:10.1007/s00203-019-01747-4 (2020). [PubMed: 31659380]
12. Reiter S & Kellogg Spadt S Bacterial vaginosis: a primer for clinicians. Postgrad Med 131, 8–18, doi:10.1080/00325481.2019.1546534 (2019). [PubMed: 30424704]
13. Onderdonk AB, Delaney ML & Fichorova RN The Human Microbiome during Bacterial Vaginosis. Clinical Microbiology Reviews 29, 223–238, doi:10.1128/cmr.00075-15 (2016). [PubMed: 26864580]
14. Reid G The development of probiotics for women's health. Canadian Journal of Microbiology 63, 269–277, doi:10.1139/cjm-2016-0733 (2017). [PubMed: 28177795]
15. Saduakhasova S et al. Lactobacillus for Vaginal Microflora Correction. Central Asian Journal of Global Health 3, doi:10.5195/cajgh.2014.171 (2014).
16. Bradshaw CS et al. Recurrence of bacterial vaginosis is significantly associated with posttreatment sexual activities and hormonal contraceptive use. Clin Infect Dis 56, 777–786, doi:10.1093/cid/cis1030 (2013). [PubMed: 23243173]
17. Balashov SV, Mordechai E, Adelson ME & Gygax SE Identification, quantification and subtyping of Gardnerella vaginalis in noncultured clinical vaginal samples by quantitative PCR. J Med Microbiol 63, 162–175, doi:10.1099/jmm.0.066407-0 (2014). [PubMed: 24200640]
18. Faught BM & Reyes S Characterization and Treatment of Recurrent Bacterial Vaginosis. J Womens Health (Larchmt) 28, 1218–1226, doi:10.1089/jwh.2018.7383 (2019). [PubMed: 31403349]
19. Schuyler JA et al. Identification of intrinsically metronidazole-resistant clades of Gardnerella vaginalis. Diagn Microbiol Infect Dis 84, 1–3, doi:10.1016/j.diagmicrobio.2015.10.006 (2016). [PubMed: 26514076]
20. Tidbury FD, Langhart A, Weidlinger S & Stute P Non-antibiotic treatment of bacterial vaginosis—a systematic review. Archives of Gynecology and Obstetrics 303, 37–45, doi:10.1007/s00404-020-05821-x (2021). [PubMed: 33025086]
21. Machado D, Castro J, Palmeira-de-Oliveira A, Martinez-de-Oliveira J & Cerca N Bacterial Vaginosis Biofilms: Challenges to Current Therapies and Emerging Solutions. Front Microbiol 6, 1528, doi:10.3389/fmicb.2015.01528 (2015). [PubMed: 26834706]
22. Maurya SK, Pathak K & Bali V Therapeutic potential of mucoadhesive drug delivery systems--an updated patent review. Recent Pat Drug Deliv Formul 4, 256–265, doi:10.2174/187221110793237529 (2010). [PubMed: 20649509]
23. Adedipe OE, Jacot TA, Thurman AR, Doncel GF & Clark MR Rapid measures of user's adherence to vaginal drug products using attenuated total reflectance Fourier transform infrared spectroscopy (ATR-FTIR) and multivariate discriminant techniques. PloS one 13, e0197906, doi:10.1371/journal.pone.0197906 (2018). [PubMed: 29799875]
24. Anstey Watkins J et al. Acceptability of and treatment preferences for recurrent bacterial vaginosis—Topical lactic acid gel or oral metronidazole antibiotic: Qualitative findings from the VITA trial. PloS one 14, e0224964, doi:10.1371/journal.pone.0224964 (2019). [PubMed: 31730666]
25. Taneva E et al. Vaginal microbiome modulates topical antiretroviral drug pharmacokinetics. JCI Insight 3, doi:10.1172/jci.insight.99545 (2018).
26. Bagnall P & Rizzolo D Bacterial vaginosis: A practical review. Jaapa 30, 15–21, doi:10.1097/01.JAA.0000526770.60197.fa (2017).
27. Vodstrcil LA, Muzny CA, Plummer EL, Sobel JD & Bradshaw CS Bacterial vaginosis: drivers of recurrence and challenges and opportunities in partner treatment. BMC Medicine 19, doi:10.1186/s12916-021-02077-3 (2021).

28. Petrina MAB, Cosentino LA, Rabe LK & Hillier SL Susceptibility of bacterial vaginosis (BV)-associated bacteria to secnidazole compared to metronidazole, tinidazole and clindamycin. Anaerobe 47, 115–119, doi:10.1016/j.anaerobe.2017.05.005 (2017). [PubMed: 28522362]
29. Bolton M, van der Straten A & Cohen CR Probiotics: potential to prevent HIV and sexually transmitted infections in women. Sex Transm Dis 35, 214–225, doi:10.1097/OLQ.0b013e31815b017a (2008). [PubMed: 18490864]
30. Bodean O, Munteanu O, Cirstoiu C, Secara D & Cirstoiu M Probiotics--a helpful additional therapy for bacterial vaginosis. J Med Life 6, 434–436 (2013). [PubMed: 24868256]
31. Larsson PG, Stray-Pedersen B, Ryttig KR & Larsen S Human lactobacilli as supplementation of clindamycin to patients with bacterial vaginosis reduce the recurrence rate; a 6-month, double-blind, randomized, placebo-controlled study. BMC Womens Health 8, 3, doi:10.1186/1472-6874-8-3 (2008). [PubMed: 18197974]
32. Recine N et al. Restoring vaginal microbiota: biological control of bacterial vaginosis. A prospective case–control study using Lactobacillus rhamnosus BMX 54 as adjuvant treatment against bacterial vaginosis. Archives of Gynecology and Obstetrics 293, 101–107, doi:10.1007/s00404-015-3810-2 (2016). [PubMed: 26142892]
33. Menard JP Antibacterial treatment of bacterial vaginosis: current and emerging therapies. International journal of women's health 3, 295–305, doi:10.2147/IJWH.S23814 (2011).
34. MacPhee RA, Hummelen R, Bisanz JE, Miller WL & Reid G Probiotic strategies for the treatment and prevention of bacterial vaginosis. Expert Opin Pharmacother 11, 2985–2995, doi:10.1517/14656566.2010.512004 (2010). [PubMed: 21080853]
35. Mastromarino P, Vitali B & Mosca L Bacterial vaginosis: a review on clinical trials with probiotics. The new microbiologica 36, 229–238 (2013). [PubMed: 23912864]
36. Chandrashekhar P, Minooei F, Arreguin W, Masigol M & Steinbach-Rankins JMPerspectives on Existing and Novel Alternative Intravaginal Probiotic Delivery Methods in the Context of Bacterial Vaginosis Infection. The AAPS Journal 23, doi:10.1208/s12248-021-00602-z (2021).
37. Yoha KS, Nida S, Dutta S, Moses JA & Anandharamakrishnan C Targeted Delivery of Probiotics: Perspectives on Research and Commercialization. Probiotics and Antimicrobial Proteins 14, 15–48, doi:10.1007/s12602-021-09791-7 (2022). [PubMed: 33904011]
38. Cook MT & Brown MB Polymeric gels for intravaginal drug delivery. Journal of Controlled Release 270, 145–157, doi:10.1016/j.jconrel.2017.12.004 (2018). [PubMed: 29223536]
39. Srikrishna S & Cardozo L The vagina as a route for drug delivery: a review. International Urogynecology Journal 24, 537–543, doi:10.1007/s00192-012-2009-3 (2013). [PubMed: 23229421]
40. Schwebke JR, Marrazzo J, Beelen AP & Sobel JD A Phase 3, Multicenter, Randomized, Double-Blind, Vehicle-Controlled Study Evaluating the Safety and Efficacy of Metronidazole Vaginal Gel 1.3% in the Treatment of Bacterial Vaginosis. Sexually Transmitted Diseases 42, 376–381, doi:10.1097/olq.0000000000000300 (2015). [PubMed: 26222750]
41. Gerton ML & Mann BK Mucoadhesive hyaluronic acid-based films for vaginal delivery of metronidazole.Journal of Biomedical Materials Research Part B: Applied Biomaterials 109, 1706–1712, doi:10.1002/jbm.b.34827 (2021). [PubMed: 33675578]
42. Malli S & et al. In situ forming pluronic® F127/chitosan hydrogel limits metronidazole transmucosal absorption. European Journal of Pharmaceutics and Biopharmaceutics 112, 143 (2017). [PubMed: 27890510]
43. Li S, Culkin A, Jones DS & Andrews GP Development of Polycaprolactone-Based metronidazole matrices for intravaginal extended drug delivery using a mechanochemically prepared therapeutic deep eutectic system. Int J Pharm 593, 120071, doi:10.1016/j.ijpharm.2020.120071 (2021). [PubMed: 33246048]
44. Singh VK & et al. Preparation and characterization of novel carbopol based bigels for topical delivery of metronidazole for the treatment of bacterial vaginosis. Materials Science and Engineering: C 44, 151 (2014). [PubMed: 25280691]
45. Tugcu-Demiröz F & et al. Electrospun metronidazole-loaded nanofibers for vaginal drug delivery. Drug Development and Industrial Pharmacy 46, 1015 (2020). [PubMed: 32393132]

46. Ndesendo VMK et al. A Review of Current Intravaginal Drug Delivery Approaches Employed for the Prophylaxis of HIV/AIDS and Prevention of Sexually Transmitted Infections. AAPS PharmSciTech 9, 505–520, doi:10.1208/s12249-008-9073-5 (2008). [PubMed: 18431651]
47. Tomás M, Palmeira-de-Oliveira A, Simões S, Martinez-de-Oliveira J & Palmeira-de-Oliveira R Bacterial vaginosis: Standard treatments and alternative strategies. Int J Pharm 587, 119659, doi:10.1016/j.ijpharm.2020.119659 (2020). [PubMed: 32687973]
48. Osmałek T et al. Recent Advances in Polymer-Based Vaginal Drug Delivery Systems. Pharmaceutics 13, 884, doi:10.3390/pharmaceutics13060884 (2021). [PubMed: 34203714]
49. Tiboni M, Campana R, Frangipani E & Casettari L 3D printed clotrimazole intravaginal ring for the treatment of recurrent vaginal candidiasis. Int J Pharm 596, 120290, doi:10.1016/j.ijpharm.2021.120290 (2021). [PubMed: 33524521]
50. Chen Y, Traore YL, Walker L, Yang S & Ho EA Fused deposition modeling three-dimensional printing of flexible polyurethane intravaginal rings with controlled tunable release profiles for multiple active drugs. Drug Delivery and Translational Research 12, 906–924, doi:10.1007/s13346-022-01133-6 (2022). [PubMed: 35211869]
51. Fu J, Yu X & Jin Y 3D printing of vaginal rings with personalized shapes for controlled release of progesterone. Int J Pharm 539, 75–82, doi:10.1016/j.ijpharm.2018.01.036 (2018). [PubMed: 29366944]
52. Tagami T, Hayashi N, Sakai N & Ozeki T 3D printing of unique water-soluble polymer-based suppository shell for controlled drug release. Int J Pharm 568, 118494, doi:10.1016/j.ijpharm.2019.118494 (2019). [PubMed: 31276763]
53. Domínguez-Robles J et al. 3D Printing of Drug-Loaded Thermoplastic Polyurethane Meshes: A Potential Material for Soft Tissue Reinforcement in Vaginal Surgery. Pharmaceutics 12, doi:10.3390/pharmaceutics12010063 (2020).
54. Utomo E & et al. Development of 3D-printed vaginal devices containing metronidazole for alternative bacterial vaginosis treatment. International Journal of Pharmaceutics: X 5, 100142 (2023). [PubMed: 36531743]
55. Arany P et al. Manufacturing and Examination of Vaginal Drug Delivery System by FDM 3D Printing. Pharmaceutics 13, 1714, doi:10.3390/pharmaceutics13101714 (2021). [PubMed: 34684007]
56. Kulinowski P et al. Development of Composite, Reinforced, Highly Drug-Loaded Pharmaceutical Printlets Manufactured by Selective Laser Sintering—In Search of Relevant Excipients for Pharmaceutical 3D Printing. Materials 15, 2142, doi:10.3390/ma15062142 (2022). [PubMed: 35329594]
57. Windolf H, Chamberlain R & Quodbach J Predicting Drug Release from 3D Printed Oral Medicines Based on the Surface Area to Volume Ratio of Tablet Geometry. Pharmaceutics 13, 1453, doi:10.3390/pharmaceutics13091453 (2021). [PubMed: 34575529]
58. Elkasabgy NA, Mahmoud AA & Maged A 3D printing: An appealing route for customized drug delivery systems. Int J Pharm 588, 119732, doi:10.1016/j.ijpharm.2020.119732 (2020). [PubMed: 32768528]
59. Chachlioutaki K et al. Quality control evaluation of paediatric chocolate-based dosage forms: 3D printing vs mold-casting method. Int J Pharm 624, 121991, doi:10.1016/j.ijpharm.2022.121991 (2022). [PubMed: 35809833]
60. Suárez-González J & et al. Individualized orodispersible pediatric dosage forms obtained by molding and semi-solid extrusion by 3D printing: A comparative study for hydrochlorothiazide. Journal of Drug Delivery Science and Technology 66, 102884 (2021).
61. Annaji M et al. Application of Extrusion-Based 3D Printed Dosage Forms in the Treatment of Chronic Diseases. J Pharm Sci 109, 3551–3568, doi:10.1016/j.xphs.2020.09.042 (2020). [PubMed: 33035541]
62. Vaz VM & Kumar L 3D Printing as a Promising Tool in Personalized Medicine. AAPS PharmSciTech 22, doi:10.1208/s12249-020-01905-8 (2021).
63. Rodríguez-López L, Shokry DS, Cruz JM, Moldes AB & Waters LJ The effect of the presence of biosurfactant on the permeation of pharmaceutical compounds through silicone membrane.

Colloids and Surfaces B: Biointerfaces 176, 456–461, doi:10.1016/j.colsurfb.2018.12.072 (2019). [PubMed: 30682618]

64. Razavi M, Primavera R, Vykunta A & Thakor AS Silicone-based bioscaffolds for cellular therapies. Mater Sci Eng C Mater Biol Appl 119, 111615, doi:10.1016/j.msec.2020.111615 (2021). [PubMed: 33321658]
65. Sołoducho J, Zając D, Spychalska K, Baluta S & Cabaj J Conducting Silicone-Based Polymers and Their Application. Molecules 26, 2012, doi:10.3390/molecules26072012 (2021). [PubMed: 33916125]
66. Tietz K & Klein S Simulated Genital Tract Fluids and Their Applicability in Drug Release/Dissolution Testing of Vaginal Dosage Forms. Dissolution Technologies 25, 40–51, doi:10.14227/dt250318p40 (2018).
67. Alauzet C, Lozniewski A & Marchandin H Metronidazole resistance and nim genes in anaerobes: A review. Anaerobe 55, 40–53, doi:10.1016/j.anaerobe.2018.10.004 (2019). [PubMed: 30316817]
68. Mahjabeen S, Hatipoglu MK, Chandra V, Benbrook DM & Garcia-Contreras L Optimization of a Vaginal Suppository Formulation to Deliver SHetA2 as a Novel Treatment for Cervical Dysplasia. Journal of Pharmaceutical Sciences 107, 638–646, doi:10.1016/j.xphs.2017.09.018 (2018). [PubMed: 28989018]
69. Romano MR & et al. Temperature Effect on Rheological Behavior of Silicone Oils. A Model for the Viscous Heating. Journal of Physical Chemistry B, The 121, 7048 (2017).
70. Bashi YHD & et al. Silicone elastomer formulations for improved performance of a multipurpose vaginal ring releasing dapivirine and levonorgestrel. International Journal of Pharmaceutics: X 3, 100091 (2021). [PubMed: 34977558]
71. Malcolm RK, Boyd PJ, McCoy CF & Murphy DJ Microbicide vaginal rings: Technological challenges and clinical development. Adv Drug Deliv Rev 103, 33–56, doi:10.1016/j.addr.2016.01.015 (2016). [PubMed: 26829289]
72. Lukin RY, Kuchkaev AM, Sukhov AV, Bekmukhamedov GE & Yakhvarov DG Platinum-Catalyzed Hydrosilylation in Polymer Chemistry. Polymers (Basel) 12, doi:10.3390/polym12102174 (2020).
73. Inglis DW A method for reducing pressure-induced deformation in silicone microfluidics. Biomicrofluidics 4, 026504, doi:10.1063/1.3431715 (2010). [PubMed: 20697573]
74. Liu X, Champagne CP, Lee BH, Boye JI & Casgrain M Thermostability of Probiotics and Their alpha -Galactosidases and the Potential for Bean Products. Biotechnol Res Int 2014, 472723, doi:10.1155/2014/472723 (2014). [PubMed: 24744923]
75. Anjum N et al. Lactobacillus acidophilus: characterization of the species and application in food production. Crit Rev Food Sci Nutr 54, 1241–1251, doi:10.1080/10408398.2011.621169 (2014). [PubMed: 24499153]
76. McCoy CF et al. Mechanical testing methods for drug-releasing vaginal rings. Int J Pharm 559, 182–191, doi:10.1016/j.ijpharm.2019.01.026 (2019). [PubMed: 30668990]
77. Rahn DD, Acevedo JF & Word RA Effect of vaginal distention on elastic fiber synthesis and matrix degradation in the vaginal wall: potential role in the pathogenesis of pelvic organ prolapse. American Journal of Physiology-Regulatory, Integrative and Comparative Physiology 295, 1351 (2008).
78. Narade S, Patil S, Surve S, Shete D & Pole Y Simultaneous UV spectrophtometric method for the determination of diacerein and aceclofenac in tables. J Pharm Sci Res 2, 137–142 (2010).
79. Mandrycky C, Wang Z, Kim K & Kim DH 3D bioprinting for engineering complex tissues. Biotechnol Adv 34, 422–434, doi:10.1016/j.biotechadv.2015.12.011 (2016). [PubMed: 26724184]
80. Perea-Lowery L, Gibreel M, Vallittu PK & Lassila L Evaluation of the mechanical properties and degree of conversion of 3D printed splint material. J Mech Behav Biomed Mater 115, 104254, doi:10.1016/j.jmbbm.2020.104254 (2021). [PubMed: 33333480]
81. Launer P, Arkles B, 2013. Infrared Analysis of Organosilicon Compounds. In: Silicon Compounds: Silanes & Silicones, 3rd Edition Gelest Inc.), Chapter: Infrared Analysis of Organosilicon Compounds, pp. 175–178.
82. Kollerup Madsen B, Hilscher M, Zetner D & Rosenberg J Adverse reactions of dimethyl sulfoxide in humans: a systematic review. F1000Res 7, 1746, doi:10.12688/f1000research.16642.2 (2018). [PubMed: 31489176]

83. Ranjit E, Raghubanshi BR, Maskey S & Parajuli P Prevalence of Bacterial Vaginosis and Its Association with Risk Factors among Nonpregnant Women: A Hospital Based Study. International Journal of Microbiology 2018, 1–9, doi:10.1155/2018/8349601 (2018).
84. Coudray MS & Madhivanan P Bacterial vaginosis-A brief synopsis of the literature. Eur J Obstet Gynecol Reprod Biol 245, 143–148, doi:10.1016/j.ejogrb.2019.12.035 (2020). [PubMed: 31901667]
85. Trenfield SJ et al. Shaping the future: recent advances of 3D printing in drug delivery and healthcare. Expert Opinion on Drug Delivery 16, 1081–1094, doi:10.1080/17425247.2019.1660318 (2019). [PubMed: 31478752]
86. Alhnan MA et al. Emergence of 3D Printed Dosage Forms: Opportunities and Challenges. Pharmaceutical Research 33, 1817–1832, doi:10.1007/s11095-016-1933-1 (2016). [PubMed: 27194002]
87. Bácskay I, Ujhelyi Z, Fehér P & Arany P The Evolution of the 3D-Printed Drug Delivery Systems: A Review. Pharmaceutics 14, 1312, doi:10.3390/pharmaceutics14071312 (2022). [PubMed: 35890208]
88. Sharma V et al. Investigations of process parameters during dissolution studies of drug loaded 3D printed tablets. Proc Inst Mech Eng H 235, 523–529, doi:10.1177/0954411921993582 (2021). [PubMed: 33570013]
89. Norman J, Madurawe RD, Moore CM, Khan MA & Khairuzzaman A A new chapter in pharmaceutical manufacturing: 3D-printed drug products. Adv Drug Deliv Rev 108, 39–50, doi:10.1016/j.addr.2016.03.001 (2017). [PubMed: 27001902]
90. Osouli-Bostanabad K & Adibkia K Made-on-demand, complex and personalized 3D-printed drug products. BioImpacts 8, 77–79, doi:10.15171/bi.2018.09 (2018). [PubMed: 29977828]
91. Forbes CJ et al. Modified Silicone Elastomer Vaginal Gels for Sustained Release of Antiretroviral HIV Microbicides. Journal of Pharmaceutical Sciences 103, 1422–1432, doi:10.1002/jps.23913 (2014). [PubMed: 24585370]
92. Fetherston SM et al. A silicone elastomer vaginal ring for HIV prevention containing two microbicides with different mechanisms of action. Eur J Pharm Sci 48, 406–415, doi:10.1016/j.ejps.2012.12.002 (2013). [PubMed: 23266465]
93. Woolfson AD, Malcolm RK & Gallagher RJ Design of a silicone reservoir intravaginal ring for the delivery of oxybutynin. Journal of controlled release : official journal of the Controlled Release Society 91, 465–476, doi:10.1016/s0168-3659(03)00277-3 (2003). [PubMed: 12932723]
94. Janusziewicz R, Mecham SJ, Olson KR & Benhabbour SR Design and Characterization of a Novel Series of Geometrically Complex Intravaginal Rings with Digital Light Synthesis. Adv Mater Technol 5, doi:10.1002/admt.202000261 (2020).
95. Rafiei F et al. Development of Hormonal Intravaginal Rings: Technology and Challenges. Geburtshilfe Frauenheilkd 81, 789–806, doi:10.1055/a-1369-9395 (2021). [PubMed: 34276064]
96. Murphy DJ et al. Impact of ring size and drug loading on the pharmacokinetics of a combination dapivirine-darunavir vaginal ring in cynomolgus macaques. Int J Pharm 550, 300–308, doi:10.1016/j.ijpharm.2018.08.051 (2018). [PubMed: 30153490]
97. Malcolm RK et al. Controlled release of a model antibacterial drug from a novel self-lubricating silicone biomaterial. Journal of controlled release : official journal of the Controlled Release Society 97, 313–320, doi:10.1016/j.jconrel.2004.03.029 (2004). [PubMed: 15196758]
98. Snorradóttir BS, Gudnason PI, Thorsteinsson F & Másson M Experimental design for optimizing drug release from silicone elastomer matrix and investigation of transdermal drug delivery. Eur J Pharm Sci 42, 559–567, doi:10.1016/j.ejps.2011.02.011 (2011). [PubMed: 21371556]
99. Snorradóttir BS, Jónsdóttir F, Sigurdsson ST, Thorsteinsson F & Másson M Numerical modelling and experimental investigation of drug release from layered silicone matrix systems. Eur J Pharm Sci 49, 671–678, doi:10.1016/j.ejps.2013.05.006 (2013). [PubMed: 23684932]
100. Rasch F et al. Macroscopic Silicone Microchannel Matrix for Tailored Drug Release and Localized Glioblastoma Therapy. ACS Biomaterials Science & Engineering 6, 3388–3397, doi:10.1021/acsbiomaterials.0c00094 (2020). [PubMed: 33463157]

101. Tolia G & Li SK Study of drug release and tablet characteristics of silicone adhesive matrix tablets. Eur J Pharm Biopharm 82, 518–525, doi:10.1016/j.ejpb.2012.07.006 (2012). [PubMed: 22820648]
102. Mazurek P, Brook MA & Skov AL Glycerol–Silicone Elastomers as Active Matrices with Controllable Release Profiles. Langmuir 34, 11559–11566, doi:10.1021/acs.langmuir.8b02039 (2018). [PubMed: 30153731]
103. Di Francesco M et al. Engineering shape-defined PLGA microPlates for the sustained release of anti-inflammatory molecules. Journal of controlled release : official journal of the Controlled Release Society 319, 201–212, doi:10.1016/j.jconrel.2019.12.039 (2020). [PubMed: 31899267]
104. Patel SK, Khoder M, Peak M & Alhnan MA Controlling drug release with additive manufacturing-based solutions. Advanced Drug Delivery Reviews 174, 369–386, doi:10.1016/j.addr.2021.04.020 (2021). [PubMed: 33895213]
105. Figueiredo S, Fernandes AI, Carvalho FG & Pinto JF Performance and paroxetine stability in tablets manufactured by fused deposition modelling-based 3D printing. J Pharm Pharmacol 74, 67–76, doi:10.1093/jpp/rgab138 (2022). [PubMed: 34591102]
106. Emmermacher J et al. Engineering considerations on extrusion-based bioprinting: interactions of material behavior, mechanical forces and cells in the printing needle. Biofabrication 12, 025022, doi:10.1088/1758-5090/ab7553 (2020). [PubMed: 32050179]
107. Stan CA, Tang SK & Whitesides GM Independent control of drop size and velocity in microfluidic flow-focusing generators using variable temperature and flow rate. Anal Chem 81, 2399–2402, doi:10.1021/ac8026542 (2009). [PubMed: 19209912]
108. Mohammed AA & et al. Optimization of semisolid extrusion (pressure-assisted microsyringe)-based 3D printing process for advanced drug delivery application. Annals of 3D Printed Medicine 2, 100008 (2021).
109. Clark JT et al. Quantitative evaluation of a hydrophilic matrix intravaginal ring for the sustained delivery of tenofovir. Journal of controlled release : official journal of the Controlled Release Society 163, 240–248, doi:10.1016/j.jconrel.2012.08.033 (2012). [PubMed: 22981701]
110. Johnson TJ et al. A 90-day tenofovir reservoir intravaginal ring for mucosal HIV prophylaxis. Antimicrob Agents Chemother 56, 6272–6283, doi:10.1128/AAC.01431-12 (2012). [PubMed: 23006751]
111. Johnson TJ, Gupta KM, Fabian J, Albright TH & Kiser PF Segmented polyurethane intravaginal rings for the sustained combined delivery of antiretroviral agents dapivirine and tenofovir. European Journal of Pharmaceutical Sciences 39, 203–212, doi:10.1016/j.ejps.2009.11.007 (2010). [PubMed: 19958831]
112. Spoerk M & et al. Personalised urethra pessaries prepared by material extrusion-based additive manufacturing. International Journal of Pharmaceutics 608, 121112 (2021). [PubMed: 34547391]
113. Eder S & et al. Toward a new generation of vaginal pessaries via 3D-printing: Concomitant mechanical support and drug delivery. European Journal of Pharmaceutics and Biopharmaceutics 174, 77 (2022). [PubMed: 35390451]
114. Herold S et al. Release Kinetics of Metronidazole from 3D Printed Silicone Scaffolds for Sustained Application to the Female Reproductive Tract. Biomedical Engineering Advances 5, 100078 (2023). [PubMed: 37123989]
115. Fanse S & et al. Effect of crosslinking on the physicochemical properties of polydimethylsiloxane-based levonorgestrel intrauterine systems. International Journal of Pharmaceutics 609, 121192 (2021). [PubMed: 34666142]
116. Fanse S & et al. Impact of polymer crosslinking on release mechanisms from long-acting levonorgestrel intrauterine systems. International Journal of Pharmaceutics 612, 121383 (2022). [PubMed: 34919997]
117. Bukhari SMH, Khan S, Rehanullah M & Ranjha NM Synthesis and Characterization of Chemically Cross-Linked Acrylic Acid/Gelatin Hydrogels: Effect of pH and Composition on Swelling and Drug Release. International Journal of Polymer Science 2015, 1–15, doi:10.1155/2015/187961 (2015).

118. Martinez AW, Caves JM, Ravi S, Li W & Chaikof EL Effects of crosslinking on the mechanical properties, drug release and cytocompatibility of protein polymers. Acta Biomater 10, 26–33, doi:10.1016/j.actbio.2013.08.029 (2014). [PubMed: 23993944]

119. Teng W, Cappello J & Wu X Physical crosslinking modulates sustained drug release from recombinant silk-elastinlike protein polymer for ophthalmic applications. Journal of controlled release : official journal of the Controlled Release Society 156, 186–194, doi:10.1016/j.jconrel.2011.07.036 (2011). [PubMed: 21839125]

120. Wang Z, Volinsky AA & Gallant ND Crosslinking effect on polydimethylsiloxane elastic modulus measured by custom-built compression instrument. Journal of Applied Polymer Science 131, n/a-n/a, doi:10.1002/app.41050 (2014).

121. Enggi CK & et al. Development of thermosensitive and mucoadhesive gels of cabotegravir for enhanced permeation and retention profiles in vaginal tissue: A proof of concept study. International Journal of Pharmaceutics 609, 121182 (2021). [PubMed: 34648879]

122. Pereira RRDA & Bruschi ML Vaginal mucoadhesive drug delivery systems. Drug Development and Industrial Pharmacy 38, 643 (2012). [PubMed: 21999572]

123. Boddupalli B & et al. Mucoadhesive drug delivery system: An overview. Journal of Advanced Pharmaceutical Technology and Research 1, 381 (2010). [PubMed: 22247877]

124. Nagahama K et al. Enhanced Immunostimulating Activity of Lactobacilli-Mimicking Materials by Controlling Size. Bioconjugate Chemistry 26, 1775–1781, doi:10.1021/acs.bioconjchem.5b00319 (2015). [PubMed: 26203868]

125. Kyser AJ et al. 2023. Fabrication and characterization of bioprints with Lactobacillus crispatus for vaginal application. J. Control. Release 357, 545–560. doi:10.1016/j.jconrel.2023.04.023. [PubMed: 37076014]

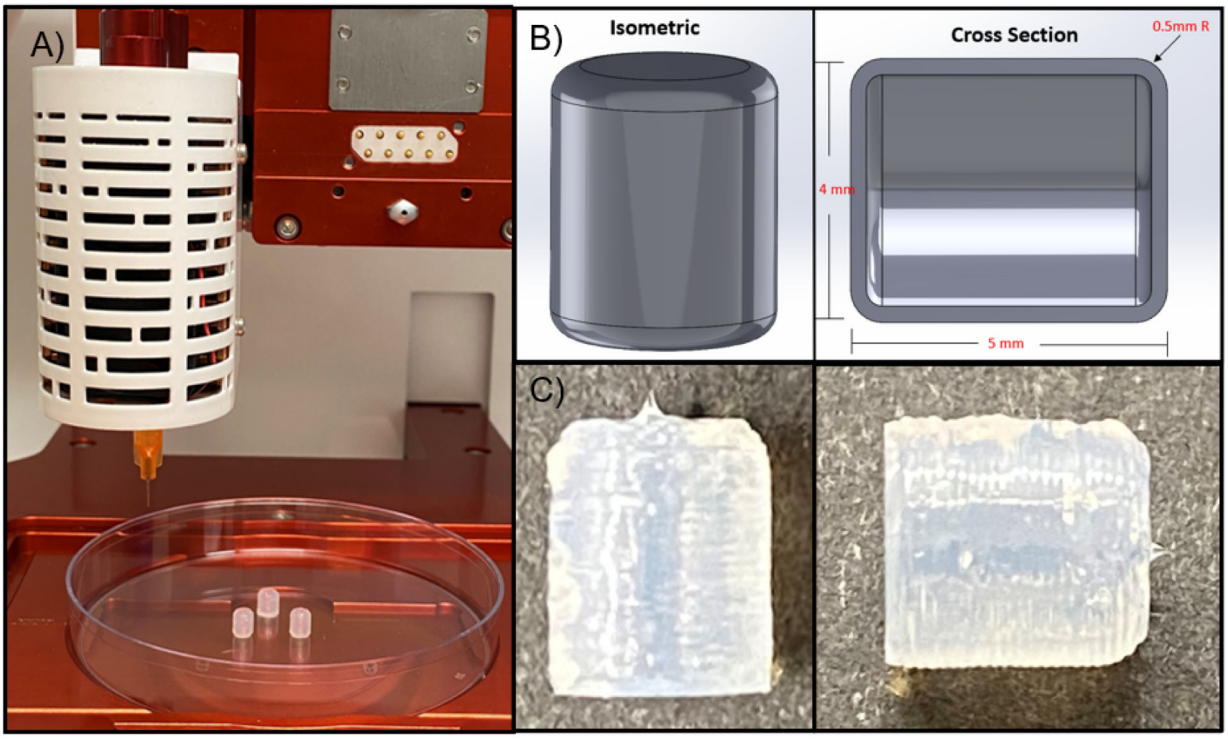

Figure 1:

(A) Vinyl terminated polydimethylsiloxane (70%) and vinyl, methyl modified silica (30%), and curing agent, methylhydrosiloxane-dimethylsiloxane copolymer, trimethylsiloxane terminated, were mixed with dimethyl sulfoxide (DMSO), and 50 μg/mg of metronidazole was loaded into the silicone ink. (B) Solidworks CAD design schematic implemented for applications in isometric and cross section view. (C) 3D-printed blank scaffold created from the STL template for reproducible dimensions of geometric design.

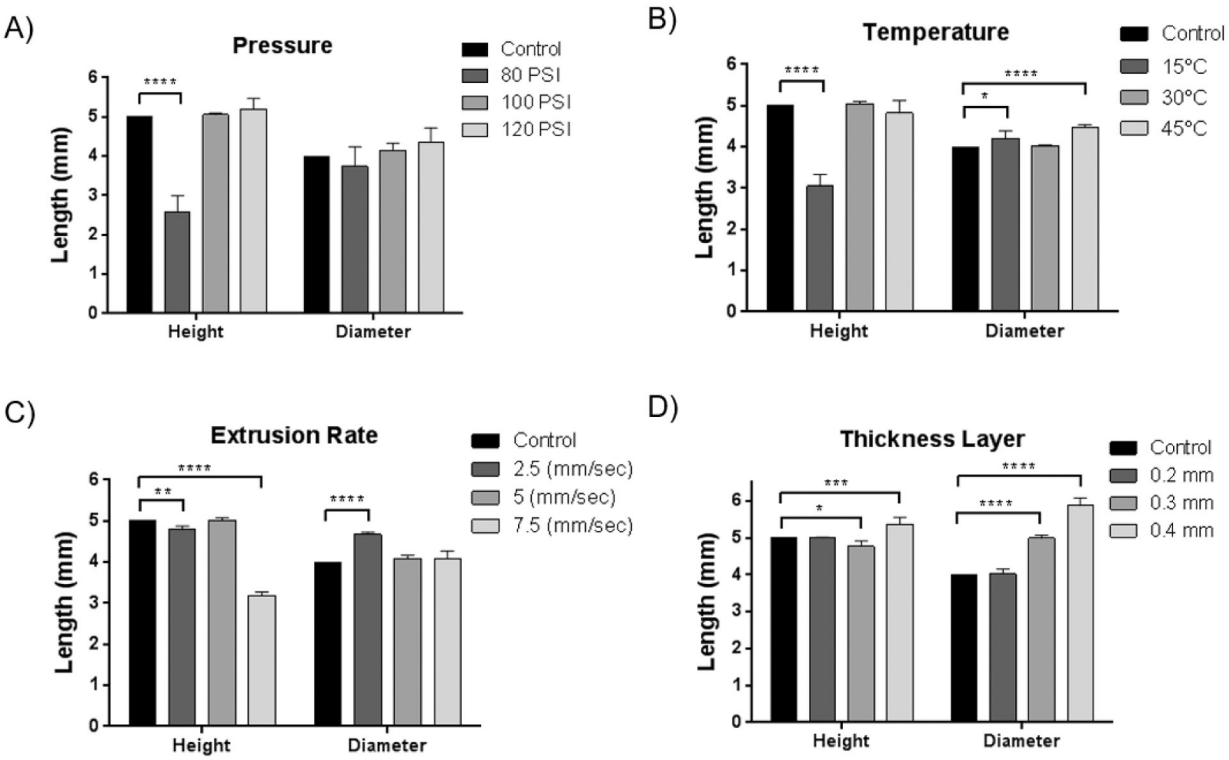

Figure 2.

Silicone scaffolds were 3D-printed at varying 3D-printing parameter values to determine most advantageous values for reproduction with accurate dimensions of height (5 mm) and diameter (4 mm) for future murine application. Dimensions were evaluated when (A) extrusion was adjusted at pressures of 80, 100, and 120 PSI, (B) temperature of CORE head was adjusted to 15, 30, and 45°C, (C) extrusion rates were varied at 2.5, 5, 7.5 mm/sec, and (D) thickness layers were 0.2, 0.3, and 0.4 mm. Statistical significance between different concentration groups and blank, as calculated by one-way ANOVA (Tukey HSD post-hoc comparisons), is represented by *$p \leq 0.05$, ** $p \leq 0.01$, ***$p \leq 0.001$ and ****$p \leq 0.0001$.

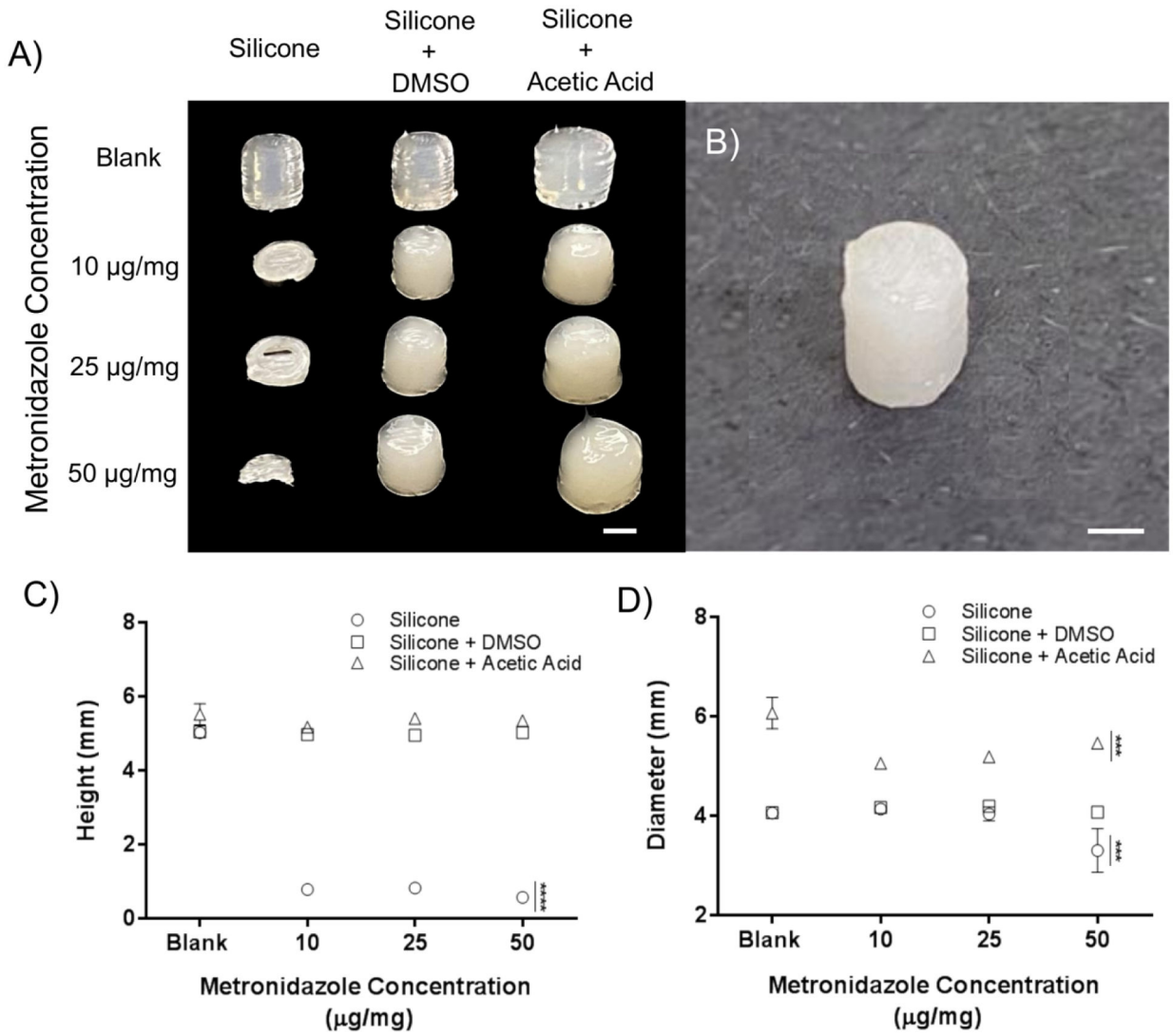

Figure 3.

3D-printing silicone ink formulations utilizing acetic acid and dimethyl sulfoxide (DMSO) were used in dissolution of metronidazole in the ink. Scaffolds were printed with 5 mm height and 4 mm diameter for future pre-clinical (murine) application. (A) Scaffold resolution was compared between formulations with metronidazole concentrations of 10, 25, 50 µg/mg in ink. (B) Representative images of ideal dimensions of metronidazole-containing scaffold. Dimensions of the different formulations when loaded at 10, 25, and 50 µg/mg were evaluated for scaffold (C) height and (D) diameter. Statistical significance between different concentration groups and blank, as calculated by one-way ANOVA (Tukey HSD post-hoc comparisons), is represented by ***$p \leq 0.001$ and ****$p \leq 0.0001$. Scale bar represents 2 mm.

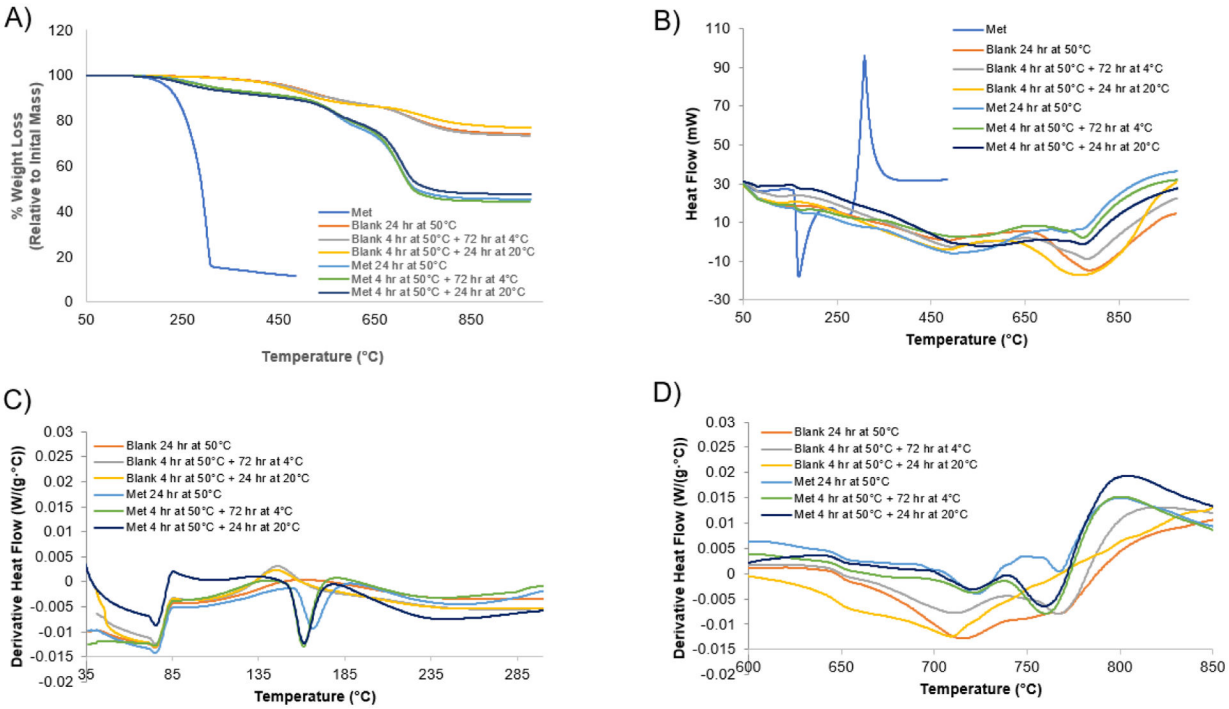

Figure 4.

3D-printed blank and metronidazole-containing silicone scaffolds at curing conditions 24 hr at 50°C, 4 hr at 50°C followed by 72 hr at 4°C, and 4 hr at 50°C followed by 24 hr at 20°C were thermally analyzed by (A) TGA and (B) DSC. Derivative heat flow acquired from DSC was analyzed to underscore thermal behavior of (C) metronidazole and the (D) silicone polymer.

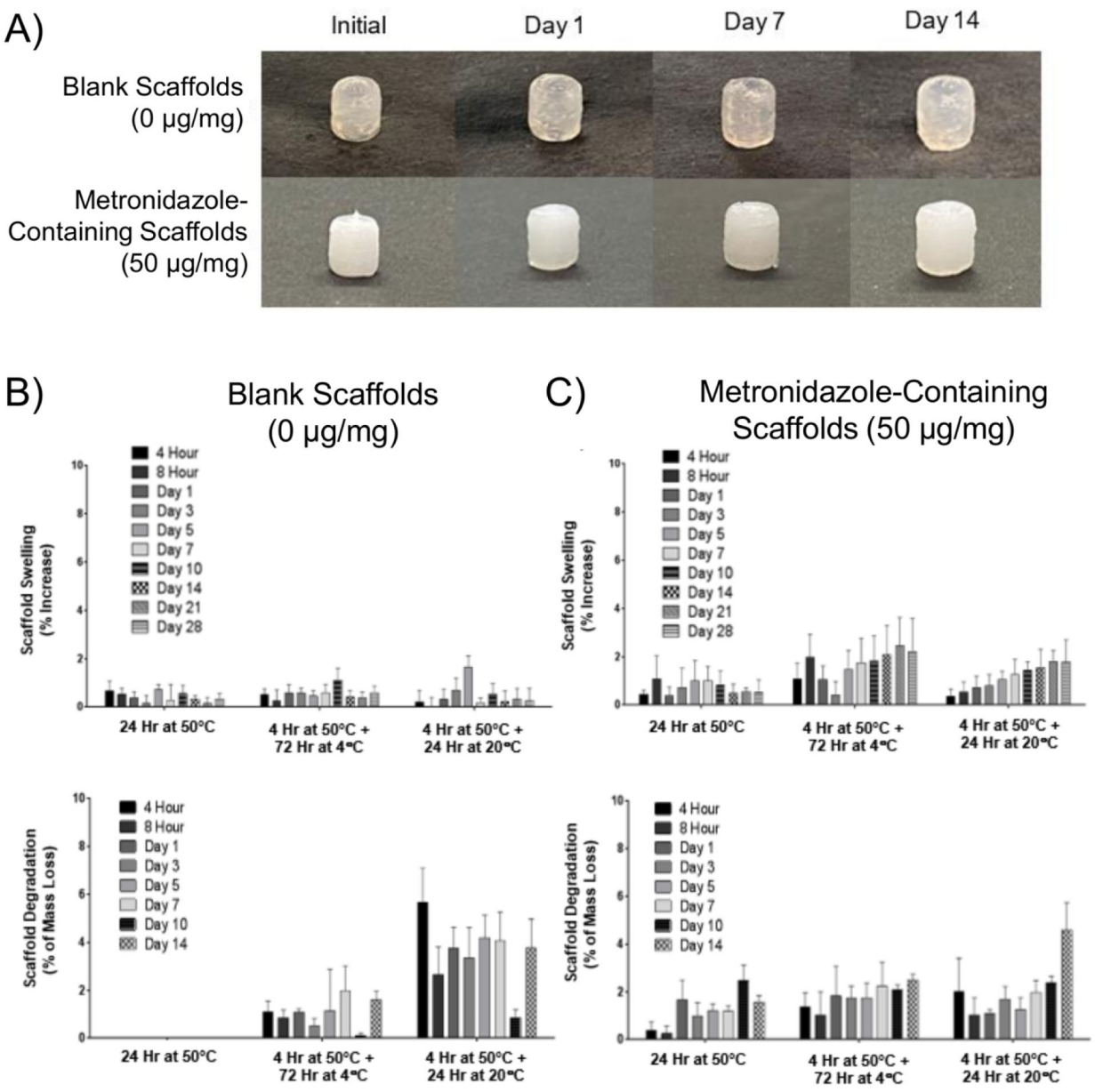

Figure 5.

Scaffold degradation and swelling were evaluated as a function of curing parameters. Representative images of (A) blank (top row) and metronidazole-containing scaffolds (bottom row) at initial post-print cure, 1, 7 and 14 days immersion in SVF. Blank and metronidazole containing scaffold (B) swelling and (C) degradation while immersed in SVF for curing parameters of 24 hr at 50°C, 4 hr at 50°C followed by 24 hr at 20°C, or 4 hr at 50°C followed by 72 hr at 4°C are shown as percent of initial mass.

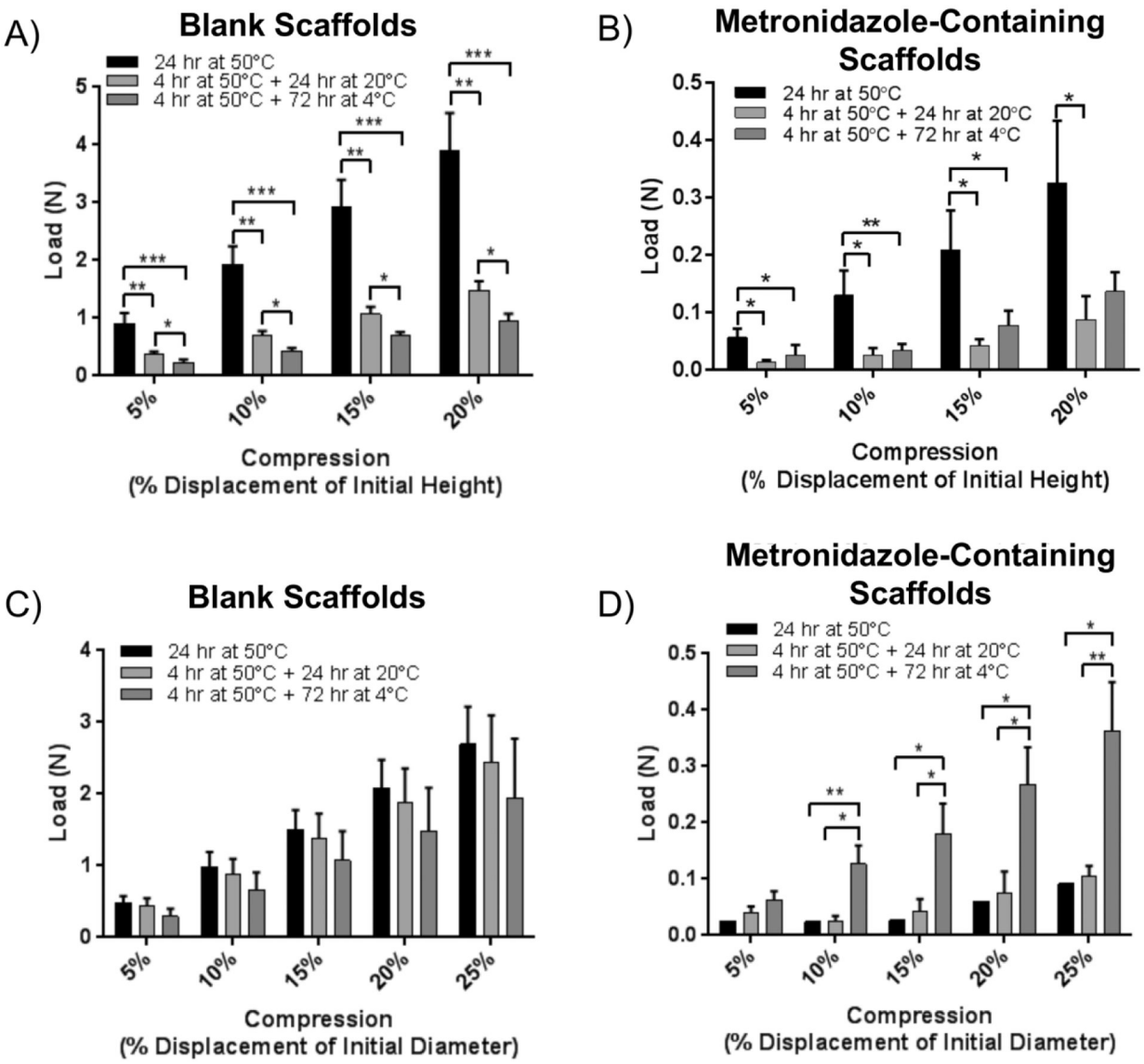

Figure 6.

Axial compression ranging from 5 to 20% was performed to simulate initial vaginal self-insertion on 3D-printed silicone (A) blank and (B) metronidazole-containing scaffolds with curing conditions of 24 hr at 50°C, 4 hr at 50°C followed by 24 hr at 20°C, or 4 hr at 50°C followed by 72 hr at 4°C post-cure. Radial compression ranging from 5 to 25% was performed after 14 days in SVF to simulate vaginal compression for duration of drug delivery on 3D-printed silicone (C) blank and (D) metronidazole-containing scaffolds with curing conditions 24 hr at 50°C, 4 hr at 50°C followed by 24 hr at 20°C, or 4 hr at 50°C followed by 72 hr at 4°C. Statistical significance between different concentration groups and blank, as calculated by one-way ANOVA (Tukey HSD post-hoc comparisons), is represented by *$p \leq 0.05$, ** $p \leq 0.01$, and *** $p \leq 0.001$.

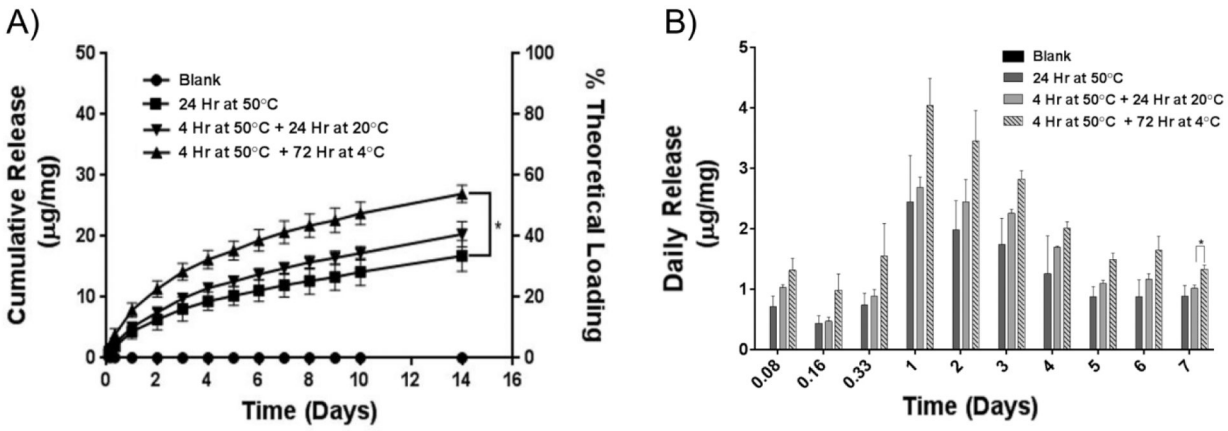

Figure 7.

Metronidazole-containing scaffolds cured at 24 hr at 50°C, 4 hr at 50°C followed by 24 at 20°C, or 4 hr at 50°C followed by 72 hr at 4°C were assessed for (A) cumulative and (B) daily release while immersed in SVF. Statistical significance between different concentration groups and blank, as calculated by one-way ANOVA (Tukey HSD post-hoc comparisons), is represented by *$p \leq 0.05$.

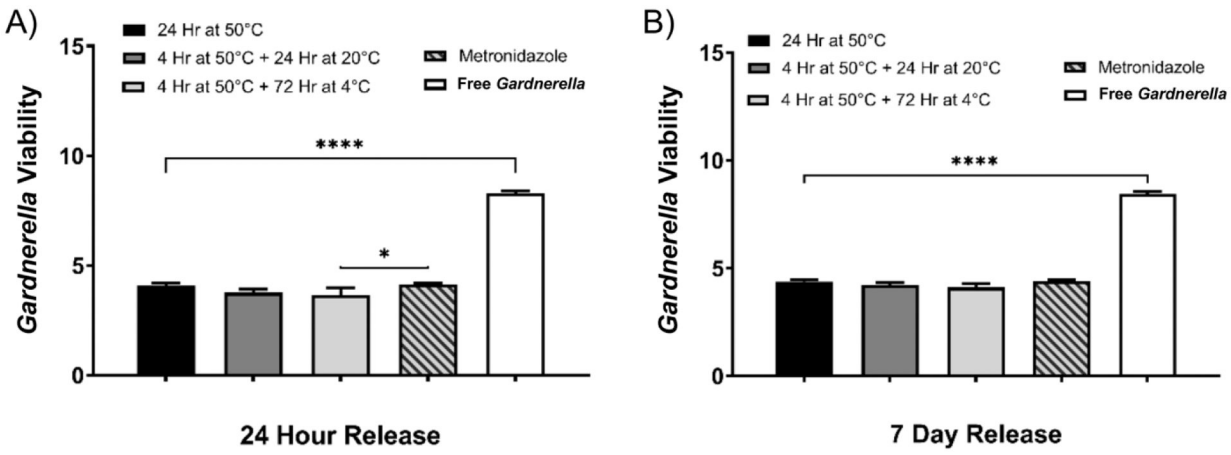

Figure 8.

Supernatant released from metronidazole-containing 3D-printed scaffolds at (A) 24 hr and (B) 7 days was added to *Gardnerella* culture for 24 hr. Viability was compared to that obtained with metronidazole alone or with free *Gardnerella* cultured with blank scaffolds. Statistical significance between experimental groups, as calculated by one-way ANOVA (Tukey HSD post-hoc comparisons), is represented by *$p \leq 0.05$ and ****$p \leq 0.0001$.

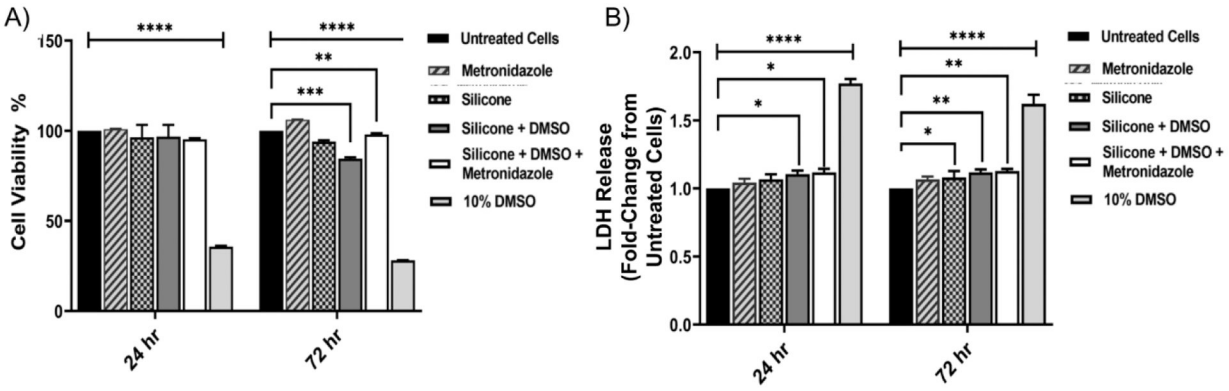

Figure 9.

Preliminary safety assessment of 3D-printed scaffolds. (A) Cell viability of vaginal keratinocytes (VK2/E6E7 cells) treated with 3D-printed scaffolds for 24 or 72 hr. Negligible cytotoxicity was observed in VK2/E6E7 cells administered with scaffolds processed with different formulations. (B) No significant release of LDH was observed from VK2/E6E7 cells treated with 3D-printed scaffolds containing silicone, silicone and DMSO, and formulation of silicone, DMSO, and metronidazole for 24 or 72 hr, relative to untreated (control) cells. In comparison, cells treated with staurosporine had significantly elevated LDH levels. Statistical significance between experimental groups, as calculated by one-way ANOVA (Tukey HSD post-hoc comparisons), is represented by * $p \leq 0.05$, ** $p \leq 0.01$, ***$p \leq 0.001$ and ****$p \leq 0.0001$.